Combining surface renewal analysis and similarity theory: A new approach for estimating sensible heat flux

F. Castellví

Department de Medi Ambient i Cienciès del Sòl, Escola Tècnica Superior Enginyeria Agrària, Universitat de Lleida, Lleida, Spain

Received 12 September 2003; revised 21 February 2004; accepted 24 March 2004; published 15 May 2004.

[1] *Castellví et al.* [2002] proposed a new approach for estimating sensible heat flux that combined surface renewal analysis and similarity theory. The approach used a calibration parameter (here referred as β) which was introduced by scaling the mean local gradient of air temperature with the ramp amplitude of air temperature over the mean volume of air parcel renewed per unit ground area, traditionally denoted as (αz), with z as the measurement height. Parameter β is explained and determined for half-hourly samples. It is shown that $(k\beta) \sim 0.1$ is appropriate under unstable conditions over a variety of canopies, with k as the von Kármán constant. This value is rather robust with regard to height and when measuring in both the roughness and inertial sublayers. This understanding of parameter β allowed a better understanding of parameter α and permitted the derivation of a modified approach for estimating sensible heat flux. In practice, it was possible to consider the new approach exempt from calibration. It was attractive for field applications and showed excellent performance under both stable and unstable conditions. A test was carried out for canopies where fetch requirements and full surface cover were not adequate. It was also shown that the flux variance method required calibration and did not perform as well as the proposed approach under such field conditions. *INDEX TERMS:* 3307 Meteorology and Atmospheric Dynamics: Boundary layer processes; 3322 Meteorology and Atmospheric Dynamics: Land/atmosphere interactions; 1818 Hydrology: Evapotranspiration; *KEYWORDS:* sensible heat flux, renewal analysis, temperature ramps, similarity theory

Citation: Castellví, F. (2004), Combining surface renewal analysis and similarity theory: A new approach for estimating sensible heat flux, *Water Resour. Res.*, *40*, W05201, doi:10.1029/2003WR002677.

1. Introduction

[2] The surface renewal theory was developed by *Higbie* [1935] to investigate interfacial heat transfer between a liquid and a gas. According to *Higbie* [1935], heat transport occurs when a "fresh fluid parcel" from the bulk fluid located above the interfacial sublayer arrives in a position adjacent to a heated surface. There is then unsteady diffusion transport during the period of contact between the parcel and the surface (the renewal frequency). This heated parcel is finally replaced by another fresh parcel from above. Advances and refinements of this theory were subsequently proposed, including models to account for the variability of the renewal frequency [*Danckwerts*, 1951] (see also *Katul et al.* [1996], summary in Table 1, and references therein). Models for describing scalar flux through the bulk transfer equation (such as those based on sensible heat and humidity fluxes over lakes and oceans) involved measuring the mean value of the scalar at the surface and at a reference height located well-above the interfacial sublayer (in the dynamic sublayer). They were developed by applying surface renewal theory at the interfacial sublayer. Part of the reason for doing this was to define (by continuity) the lower boundary conditions at the dynamic sublayer; where similarity theory is valid. This made it possible to explain the vertical profile of the scalar between the surface and a specific reference height, and the bulk transfer coefficient [*Brutsaert*, 1975; *Liu et al.*, 1979; *Soloviev and Schlüssel*, 1994; *Clayson et al.*, 1996].

[3] *Paw U and Brunet* [1991] and *Paw U et al.* [1995] used the surface renewal (SR) abstraction in conjunction with observed ramp-like patterns in the temperature time series to estimate sensible heat flux over a variety of vegetated surfaces. At the atmospheric surface layer, the analysis of such scalar patterns or features in traces has been the subject of intensive research because they are associated with organized large-scale eddy motions [*Paw U*, 2002; and references therein]. As a consequence, the renewal process can be visualized in the time series even when measuring well above a vegetated surface. In the last decade, SR analysis has been used for estimating sensible heat flux. Some of the reasons for this interest are practical: its low cost (only a fine-wire thermocouple is needed) and simplicity (it only requires temperature measurements at one height) maximize the possibility of obtaining replications. Furthermore, thermocouples can be located in places with limited or difficult access, such as within dense canopies where a sonic anemometer would not operate and over tall canopies [*Katul et al.*, 1996; *Chen et al.*, 1997a; *Spano et al.*, 2000]. The SR can therefore be used for estimating sensible heat flux and thereafter may be useful for deter-

0043-1397/04/2003WR002677

Table 1. Physical and Aerodynamic Properties for a Variety of Canopies[a]

Canopy	h, m	δ	U_h/U_*	$(z^*/h)_{0.1}$	$(z^*/h)_{0.2}$	$(z^*/h)_{0.3}$
WT strips	0.06	0.23	3.3			
Wheat	0.047	0.471	3.6			
WT rods	0.19	1	5.0			
Corn	2.6	1.5	3.6			
Corn	2.25	1.45	3.2			
Eucalypt	12	0.5	2.9	1.36	2.72	4.08
Pine	20	2.05	2.5	1.17	2.34	3.52
Aspen	10	1.95	2.6	1.22	2.44	3.66
Pine	15	1	2.2	1.03	2.06	3.09
Spruce	12	5	2.4	1.12	2.25	3.38
Spruce	12	5.1	4.0	1.87	2.75	5.63
Deciduous	24	2.5	2.8	1.31	2.62	3.94

[a]These correspond to near-neutral conditions and for a rather homogeneous canopies. WT and δ denote wind tunnel experiments and roughness density or frontal area index which is assumed to be half the single-sided leaf area index for field canopies, respectively; for further details, see *Raupach et al.* [1996, Table 1, and references therein]. The ratio z^*/h was determined for tall ($h > 12$ m) and crown dense canopies using different values for coefficient a, $(z^*/h)_a$, and setting $\alpha = 0.5$. See text.

mining latent heat flux as a residual from the surface energy balance equation when net surface flux is either measured or estimated. This may provide an inexpensive and practical method that can be useful for evaporation studies [*Snyder et al.*, 1996; *Spano et al.*, 2000].

[4] An important part of this SR research centered on improving comprehension of the parameter α (see equation (1) below). The next section presents experimental evidence about this need since when measuring well above a canopy the parameter α appears to be a nonrobust constant and can thus limit the SR utility. *Castellví et al.* [2002] derived a new approach for estimating sensible heat flux by combining surface renewal and Monin-Obukhov similarity concepts. The proposed approach depends on parameter β (see equation (2) below), but also from wind speed. The most interesting aspect of this approach is that parameter β proves to be rather conservative for both the roughness and inertial sublayers with results varying slightly for different canopies. The approach is attractive for field applications as it permits air temperature measurement at reasonable frequencies over canopies absorbing high rates of momentum; furthermore, it is not necessary to determine a ramp frequency. In general, parameter β can be assumed constant under unstable conditions and consequently, the approach proposed by *Castellví et al.* [2002] can be considered, in practice, exempt from calibration under unstable conditions.

[5] The objective of this paper is to explain parameter β. It is shown that understanding it facilitates comprehension of both the original SR and *Castellvi et al.* [2002] approaches for estimating sensible heat flux. Parameters α and β are closely related, and thus this research also contributes to a better understanding of parameter α. Here, we warn of the limitations in calibrating the parameter α for estimating sensible heat flux when measurements are taken above a canopy. A modified approach for estimating sensible heat flux is also derived, which is exempt from calibration regardless of stability conditions and measurement height. The flux variance method for estimating sensible heat flux was implemented for purposes of comparison. This method has been the subject of intensive research over the last three decades. It has been contrasted with other methods and shown to work well for different field applications [*Tillman*, 1972; *Weaver*, 1990; *Lloyd et al.*, 1991; *DeBruin et al.*, 1993; *Padro*, 1993; *Albertson et al.*, 1995; *Katul et al.*, 1995, 1996; *Wesson et al.*, 2001].

[6] It is shown that the new derived approach, which also requires wind speed measurements, performed better than the one proposed by *Castellvi et al.* [2002] and the flux variance method for different canopies (grass, wheat and grapevines). However, the free convection limit of the new derived approach holds true for slightly unstable conditions and also performs well. Hence under unstable conditions a new equation is derived that makes it possible to estimate sensible heat flux when measuring within the roughness and inertial sublayers and that requires only temperature measurements as input.

2. Theory

2.1. Background

[7] During the last decade, the SR concept appeared to be a feasible method for estimating sensible heat flux over vegetation. This SR model introduced by *Paw U et al.* [1995] is based on the fact that most of the turbulent transfer, both within and above canopies, is associated with large-scale coherent eddies that are evident as ramp-time scalar series. Figure 1 shows the time series for air temperature measured 1.5 m above (0.1m high) grass, using a fine-wire (0.0127 mm diameter) thermocouple at 10 Hz, for both unstable and stable conditions. SR analysis assumes that turbulent exchange on any scalar is driven by the regular replacement of an air parcel in contact with the sinks and sources in the surface where the exchange occurs. One air parcel sweeps down to the surface and replaces another that is ejected from the canopy. When air temperature measured at high frequency is plotted against time, the constant air renewal can be inferred from a sawtooth pattern, or series of ramps as shown in Figure 1. An ideal and comprehensive scheme for this process over vegetated surfaces (scheme 1, see Figure 2a) was originally presented by *Paw U et al.* [1995]. Under unstable conditions, a typical temperature ramp is characterized by an increase in temperature as the air parcel is heated from contact with the sources of heat within the canopy. This happens for a period of time (L_r) and is followed by a sharp, steep drop in temperature associated with the near instantaneous entry of cooler air from above. This is then followed by a quiescent period (L_q) in which there is no heating or cooling until the new parcel starts to heat again. Under stable conditions, an air parcel cools as heat is transferred to the canopy elements. A warm air parcel then sweeps in from above to replace the parcel that was previously in contact with the surface. This is followed by another quiescent period. *Chen et al.* [1997a] proposed another scheme (i.e., scheme 2, see Figure 2b). This considers a finite microfront with duration (L_f) instead of a sudden sharp steep-drop in temperature and assumes a negligible quiescent period in order to reduce numerical complexity. The quiescent period exists, but when the idealized ramp shown in scheme 2 accounts for the quiescent period between the microfront and formation of the following ramp, there were no significant improvements in sensible heat flux estimates.

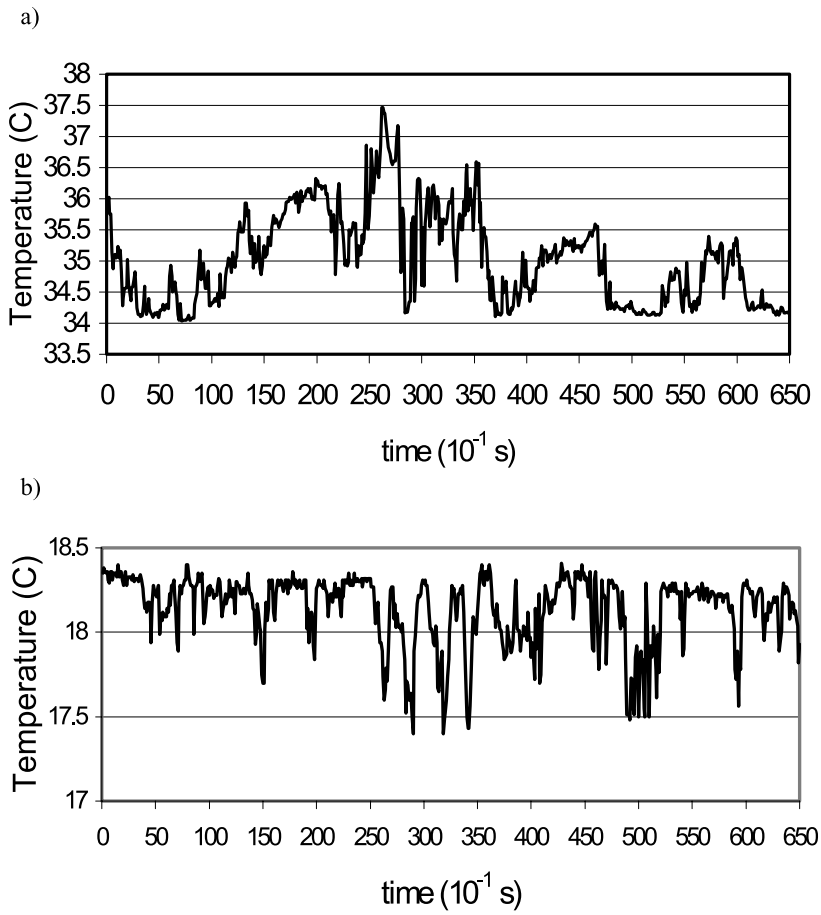

Figure 1. Ramps observed in air temperature traces. The measurements were made at a height of 1.5 m above grass (0.1 m tall) under (a) unstable conditions and (b) stable conditions.

[8] For a given period (typically half an hour) the sensible heat flux at any height is the net exchange of heat conducted by all the ramps formed during this period. Regardless of the ramp scheme used in Figure 2, if the internal temperature advection in the air parcel that is being renewed is negligible, sensible heat flux from the surface at height z (within the canopy or in the roughness and inertial sublayers) is determined by the following expression based on

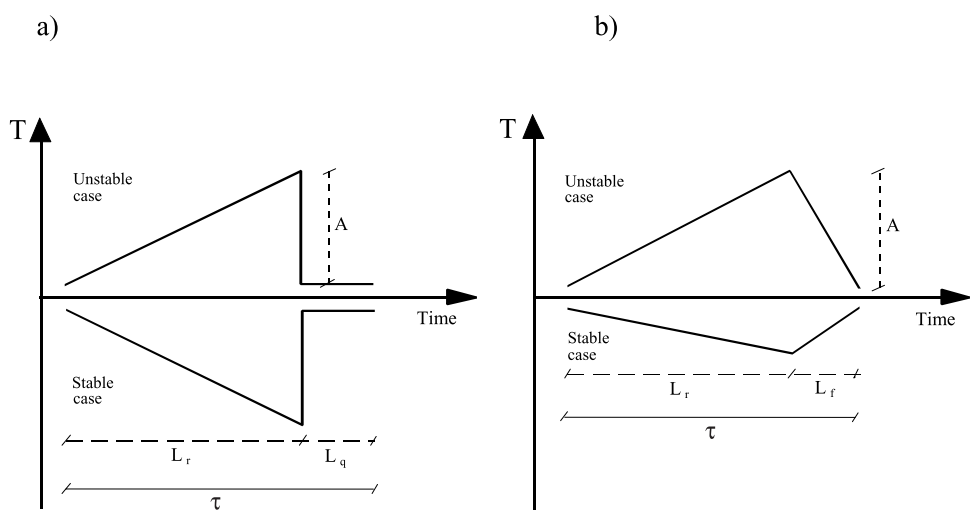

Figure 2. Ramp models (a) assuming a sharp instantaneous drop in temperature and (b) assuming a finite microfront. L_r, L_q, and L_f denote the warming, quiescent, and microfront periods, respectively. A is the ramp amplitude, and τ is the total ramp duration.

the scalar conservation equation [*Paw U et al.*, 1995; *Snyder et al.*, 1996; *Katul et al.*, 1996; *Chen et al.*, 1997a]:

$$H = (\alpha z)\rho C_p \frac{\delta T}{\delta t} = (\alpha z)\rho C_p \frac{A}{\tau} \quad (1)$$

where T, ρ and C_p are the mean temperature, density and specific heat of air at constant pressure, respectively. The required dimensions for the coherent structure in (1): A and τ (see Figure 2) are respectively the mean ramp amplitude and the inverse ramp frequency over the averaging period (algorithms for determining ramp dimensions following Figure 2b are provided in Appendix A). The variable (αz) is the averaged volume of air per unit ground area exchanged for each ramp during a given sample period and is assumed that this volume scales with z. It should be stated that little is known about the α parameter, particularly under stable conditions. It is not therefore possible to provide general rules based on previous research into different aspects of the α parameter, such as the variability of averaged or calibrated values, or its dependence on measurement height, canopy type and stability conditions. There follows a brief summary of current knowledge, but without considering the different numerical methods used to determine ramp dimensions when measurements are not made within the canopy.

[9] Several studies, most of which were conducted under unstable conditions, showed that when using the ramp model shown in Figure 2a, the value of the calibrated α parameter was approximately 0.5 when measuring at the top of a canopy and over tall vegetation [*Paw U et al.*, 1995; *Katul et al.*, 1996]. When measuring well above a canopy, this value approached unity in the inertial sublayer [*Snyder et al.*, 1996; *Spano et al.*, 1997; *Zapata and Martinez-Cob*, 2001]. In equation (1) it is assumed that the air parcel being renewed is uniformly heated and the parameter α may be interpreted as a factor that corrects for the nonuniform heating of the renewed air parcel. Following *Paw U et al.* [1995], when measuring at the canopy top, $\alpha \sim 0.5$ corrects for the unequal temperature from the bottom to the top of the renewed air parcel volume. When measuring well above the canopy, turbulence leads to quasi-uniform heating and $\alpha \sim 1$, indicating that the temperature correction in the air parcel has less weight due to the diminished internal temperature gradient [*Snyder et al.*, 1996; *Spano et al.*, 1997; *Zapata and Martinez-Cob*, 2001]. Using Figure 2b and based on samples mainly collected under unstable conditions, *Chen et al.* [1997b] found that the calibrated value for α was nearly independent of measurement height, within the canopy and in the roughness and inertial sublayers. It did, however, vary slightly between canopies and when the different levels of measurement above the canopy were relatively close. The calibrated α values obtained were close to 0.5 (ranging from 0.465 to 0.55) when measurements were mainly taken in the roughness sublayer of different types of canopies (straw mulch and Douglas fir forest), and close to 0.7 (ranging from 0.663 to 0.724) in the case of bare soil. Results derived from the different ramp models were not comparable because the ramp dimensions were different. This was particularly so when determining the ramp duration, because values corresponding to scheme 1 were approximately twice those determined using scheme 2 [*Chen et al.*, 1997a]. When using the ramp model in scheme 2, air temperature had to be measured at very high frequency (80 Hz) because of the short duration of the microfront.

[10] As mentioned above, most studies did not present clear analyses for parameter α under stable conditions because the samples collected were mixed with others obtained under unstable conditions. To the best of our knowledge, only *Paw U et al.* [1995] have applied linear fitting analyses to evaluate the performance of equation (1) exclusively under stable conditions with measurements made at the canopy top. These results suggest that values obtained for parameter α tend to be about half the magnitude of those obtained under unstable conditions for the same canopy. After filtering, the corresponding calibrated α values for unstable and stable conditions at the canopy top were: 1.25 and 0.5 for maize (2.6 m high), 0.7 and 0.33 over a walnut orchard (6 m) and 0.5 and 0.32 for tall forest (18.43 m), respectively. Regardless of the ramp model used in Figure 2 and the method for determining ramp dimensions, when measuring in the roughness sublayer under unstable conditions, the trend for parameter α versus the measurement level tended to slightly diminish with increasing measurement height.

[11] There has been little research into values for parameter α when measurements are made in the inertial sublayer under stable conditions. However, experiments over short canopies using the ramp model in scheme 1, over 0.1 m high grass [*Snyder et al.*, 1996; *Spano et al.*, 1997], over natural vegetation (0.05 m) with a high portion of bare soil [*Zapata and Matinez-Cob*, 2001], suggested that calibrated α values decrease as measurement height increases.

[12] For practical field applications, it is often desirable to made measurements well above a surface; this makes it possible to maintain the same measurement height for growing canopies and to measure at a reasonable frequency when the shear stress is large. Unless measurements are made at very high frequency, it is often difficult to detect well-formed ramp events close to short canopies in windy conditions. However, the higher the measurement frequency, the finer the thermocouple wire is required and consequently the greater the risk of thermocouple damage. Furthermore, the large amount of data that needs to be collected reduces the attractiveness of SR for practical field applications. To summarize, equation (1) generally requires specific calibration and for practical purposes it is often best not to measure too close to the canopy top, however, it is also necessary for measurements to be taken below the inertial sublayer in order to maintain its attractiveness.

[13] The ramp-like structures observed in a given period account for most of the vertical transport and consequently fit the local gradient of the scalar. This can be described in the following manner: an air parcel descends to the plant canopy from a given height with a given scalar value. Once the air parcel has descended to the canopy and begins to be enriched or depleted by the scalar, the scalar time course reflects the slow change in part of the ramp, defining the amplitude (A). If we subtract the base scalar value (see Figure 2a) which we take as representing that of the scalar at the typical height from which the air parcel originated (quiescent period), then the ramp amplitude (A) should be directly proportional to the mean temperature difference

between the original parcel height and the height at which net heat sources are located within the canopy. Following this logic, as parameter (αz) in equation (1) represents the effective eddy size of renewed air parcels with frequency τ, the following relationship was proposed by *Castellví et al.* [2002]:

$$\begin{array}{ll} \text{Inertial sublayer} & \dfrac{A}{\alpha z} \propto \dfrac{\partial T}{\partial z} = \beta \dfrac{A}{(z-d)} \\ \text{Roughness sublayer} & \dfrac{A}{\alpha z} \propto \dfrac{\partial T}{\partial z} = \beta \dfrac{A}{z} \end{array} \tag{2}$$

Where T, β and d are respectively the mean air temperature, a scale or link parameter, and the zero-plane displacement height. When measuring in the inertial sublayer, the upper boundary in (2) is given by site-specific fetch conditions.

[14] From K-theory, the sensible heat flux can be estimated as: $H = \rho C_p K_h \delta T/\delta z$, where K_h is the turbulent eddy diffusivity for heat. When combined with (2), the following expression can be derived for estimating sensible heat flux,

$$\begin{array}{ll} \text{Inertial sublayer} & H = \rho C_p \beta K_h A/(z-d) \\ \text{Roughness sublayer} & H = \rho C_p \beta K_h^* A/z \end{array} \tag{3}$$

where K_h^* is an appropriate eddy diffusivity for heat in the roughness sublayer. Monin-Obukhov similarity theory can be used over a homogeneous surface when measurements are taken in the inertial sublayer. A suitable expression for K_h is

$$K_h = k u_* (z-d) \phi_h^{-1}(\zeta) \tag{4}$$

where $k \sim 0.4$ is the von Kármán constant, u_* the friction velocity and $\phi_h(\zeta)$ the stability function for heat as defined below in equation (6). Denoting $\phi_h^*(\zeta)$ as an appropriate stability function for heat in the roughness sublayer, *Cellier and Brunet* [1992] found the ratio $\phi_h^*(\zeta)/\phi_h(\zeta) = K_h/K_h^* \sim (z\text{-}d)/z^*$, where z^* denotes the depth of the roughness sublayer.

[15] Therefore the eddy diffusivity for heat in the roughness sublayer can be estimated using the following expression:

$$K_h^* = \frac{K_h^*}{K_h} K_h = k z^* u_* \phi_h^{-1}(\zeta) \tag{5}$$

A widely accepted formulation [*Businger et al.*, 1971] for $\phi_h(\zeta)$ is

$$\begin{array}{ll} \text{Unstable} & \phi_h(\varsigma) = \left[0.74/\sqrt{1-9\,\varsigma}\right] \\ \text{Neutral} & \phi_h(\varsigma) = [0.74] \\ \text{Stable} & \phi_h(\varsigma) = [0.74 + 4.7\,\varsigma] \end{array} \tag{6}$$

where ζ is the stability parameter or a dimensionless buoyancy parameter defined as, $\zeta = (z\text{-}d)/L_o$, and L_o is the Obukhov length, which can be expressed as

$$L_o = -\rho C_p \frac{u_*^3}{kgH} T \tag{7}$$

where g is the acceleration due to gravity. *Castellví et al.* [2002] proposed estimating sensible heat flux when measuring well above the canopy by combining equations (3) and (4) to yield

$$H = \rho c_p \beta_1 A u * \phi_h^{-1}(\zeta) \tag{8}$$

The attractiveness of equation (8) was that: it also performed well when measuring in the roughness sublayer; it only required ramp amplitude as input and avoided possible errors when determining ramp frequency; and it was almost exempt from calibration, because $\beta_1 = k\,\beta \sim (0.1-0.15)$ regardless of measurement height (in the roughness and inertial sublayers) for different canopy types. However, calibration was carried out using a data set in which the samples were mainly acquired under unstable conditions. Therefore parameter β was almost constant with height. Calibrated β values obtained for different heights were as follows: $\beta \sim 0.25$, measuring in the inertial sublayer over (0.1 m high) grass; $\beta \sim 0.25$ and $\beta \sim 0.37$, measuring in the roughness sublayer over (0.7 m high) wheat and (2 m high) grapevines (with 65% ground cover), respectively. These β values were obtained by a linear fit through the origin using actual sensible heat flux from a one-dimensional sonic anemometer. Here, having determined parameter β for each sample, it is shown that $\beta \sim 0.25$ was applicable under unstable conditions.

[16] Wind speed is required to solve (8) as it is necessary to determine both the friction velocity and stability parameter, but a cup anemometer is not expensive. The typical iteration method can be used to solve (8), see method 1 in Appendix D. Similarity theory provides a set of established approaches for determining sensible heat flux from temperature and wind speed measurements, but these are often limited by fetch requirements.

2.2. Explaining Parameter β

[17] Over a homogeneous surface, turbulent heat transfer is predominantly vertical. This may therefore be described by a one-dimensional diffusion equation,

$$\frac{\partial T}{\partial t} = \frac{\partial}{\partial z}\left(K_h \frac{\partial T}{\partial z}\right) \tag{9}$$

where T is the mean air temperature and t denotes time. Given an initial air temperature profile, assuming K_h as a constant and taking z as the actual measurement height above the surface for which (9) is valid, it is possible to link the vertical gradient with the mean air temperature history at the same height z (see Appendix B),

$$\frac{\partial T_{(z,t)}}{\partial z} = \frac{2}{\sqrt{\pi K_h}} \int_{t_0}^{t} \frac{\partial T_{(z,s)}}{\partial s} d\left(\sqrt{(t-s)}\right) \tag{10}$$

where s is the integration variable. Equation (10) assumes that K_h is constant throughout the period $(t - t_0)$ and that neutral conditions are met at t_0. When using SR analysis the temperature time pattern shown in Figure 1 may be abstracted as the sum of a coherent temperature part (a well-defined ramp abstracted as shown in Figure 2) and a random temperature part. The temperature ramps (see Figure 1) represent injections of sensible heat flux into the air across a horizontal plane located at the measurement height. A net injection of sensible heat is fully represented

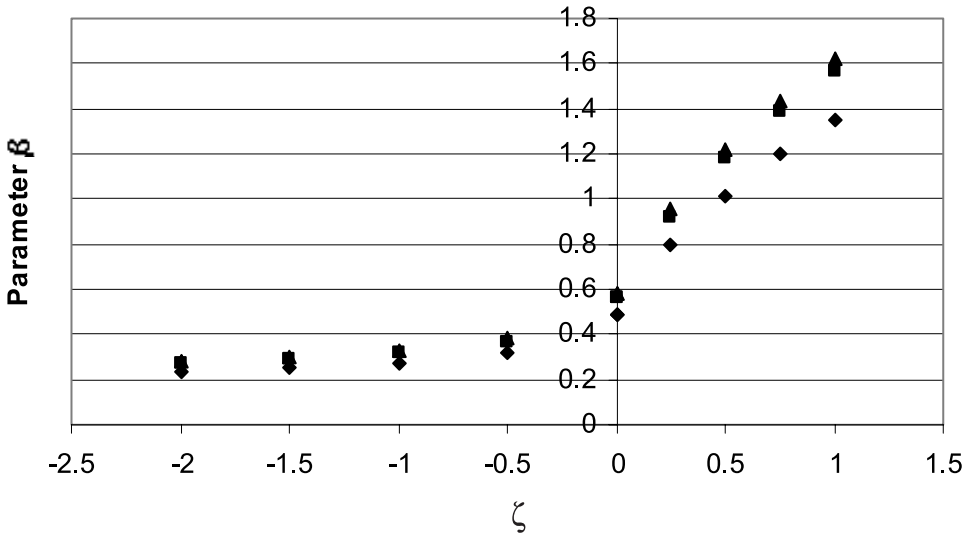

Figure 3. The parameter β, equation (12), stability parameter relationship for bare soil (diamonds), straw mulch (squares) and Douglas fir forest (triangles).

by the well-defined ramp (coherent part). In SR analysis, following *Van Atta* [1977] and *Chen et al.* [1997a], it is assumed that the temperature signal shown in Figure 1 over a period $(t - t_0)$ can be abstracted as a number of N identical ramps characterized by A and τ, with (t-to) = N τ. Consequently, the coherent structure is assumed to be the only net part that (1) fits the mean air temperature gradient evaluated at the measurement height and (2) varies the mean air temperature over time at the measurement height.

[18] It follows that only the coherent part of temperature should be taken in equation (10). Equation (1) assumes that the temperature advection term is negligible therefore the local and total derivatives are assumed to be the same over time. Over a homogeneous surface, K-Theory relates the flux of a scalar with the corresponding mean vertical gradient through a constant turbulent eddy diffusivity. Hence equations (2) and (10) can be related in order to explore a possible link between SR and similarity concepts (an explanation for parameter β). In Appendix C, there is a derivation for obtaining an expression for parameter β combining equations (2) and (10), see equation (11) below. It also presents an alternative route for obtaining equation (11) after combining equation (2) with a simplified temperature variance budget equation. Ultimately, this alternative route requires experimental verification as shown in the results section.

[19] According to equation (C8), parameter β can be expressed as

$$\beta = \begin{cases} \left[\dfrac{(z-d)}{k\pi}\,\dfrac{\phi_h(\zeta)}{\tau u_*}\right]^{1/2} & \text{if } (z-d) > z^* \\ \left[\dfrac{z^2}{k\pi z^*}\,\dfrac{\phi_h(\zeta)}{\tau u_*}\right]^{1/2} & \text{if } h \le (z-d) \le z^* \end{cases} \tag{11}$$

Equation (11) should be consistent with the performance described in section 2.1. The square root dependence on height and other variables produces close calibrated β values when the distance between measurement heights is not significant. This explains the unexpectedly weak dependence of parameter β with respect to measurement height. On the basis of ramp frequency scales with wind shear, *Chen et al.* [1997b] respectively scaled $1/(\tau u_*)$ over z or (z-d) in the roughness and inertial sublayers using a coefficient λ. Introducing the corresponding scale into equation (11) produces an expression that is independent of z for the inertial sublayer and a slightly dependent expression for the roughness sublayer,

$$\beta = \begin{cases} \left[\dfrac{\lambda\phi_h(\zeta)}{k\pi}\right]^{1/2} & \text{if } z > z^* \\ \left[\dfrac{\lambda\phi_h(\zeta)}{k\pi}\,\dfrac{z}{z^*}\right]^{1/2} & \text{if } h \le z \le z^* \end{cases} \tag{12}$$

The λ values determined for different surfaces of *Chen et al.* [1997b] were used in equation (12) to qualitatively analyze the performance of β for a range of stability conditions. When measuring over bare soil at height z = 0.03 m, straw mulch (0.06 m thick) at z = 0.09 m and Douglas fir forest (16.7 m) at z = 23 m, the λ values obtained were 0.4, 0.54 and 0.70, respectively. The results are shown in Figure 3 and are canopy-specific and valid for a fixed measurement height. In Figure 3, z^*/h, with h as the canopy height, was set to $z^*/h \sim 5/3$. The zero plane displacement for homogeneous canopy is $d \sim 2/3h$ [*Brutsaert*, 1982]. Then, the roughness layer depth may be estimated as $z^* = h + 2(h-d) \sim 5/3h$ [*Sellers et al.*, 1986]. Thus the measurement height for bare soil was in the inertial sublayer; for straw mulch it was near the roughness-inertial layer transition; and for Douglas fir forest it was in the roughness sublayer. Figure 3 shows that under unstable conditions, $-2 \le \zeta \le 0$, the β values fell within the following ranges: (0.23 to 0.48), (0.26 to 0.56) and (0.27 to 0.58) for bare soil, straw mulch and Douglas fir forest, respectively. Under moderately to very unstable conditions the β values tended to remain constant at around 0.25, regardless of measurement height in the inertial sublayer and type of surface.

[20] Under stable conditions β values may vary considerably. Figure 3 suggests that a general calibration of β is not recommended because a few samples under stable conditions can easily distort a suitable averaged value under unstable conditions. A very rough calibration can be expected under stable conditions when the stability parameter range at the experimental site is sufficiently wide. The tendency shown in Figure 3 confirms the calibrated β values given by *Castellví et al.* [2002] over grass, wheat and grapevines, because the samples were mainly acquired under unstable conditions. As a general rule, from Figure 3, it is inferred that when working under unstable conditions an appropriate mean β value should be close to 0.25 for any measurement level and homogeneous canopy. Hence, although only qualitatively, Figure 3 explains the temptation mentioned by *Castellví et al.* [2002] to suggest $(k\beta) \sim 0.1$ as a universal value for full ground cover and homogeneous vegetation. Our results show that under unstable conditions, $\beta \sim 0.25$, was a suitable choice for very different canopy types.

[21] *Raupach et al.* [1989, 1996], *Paw U et al.* [1992], and *Shaw et al.* [1995] have shown that ramp frequency scales with horizontal mean wind speed at the canopy top (u_h) for canopies of various heights, $1/\tau \sim a\, u_h/h$, where a is a canopy specific-constant that increases with wind shear and falls within the range, $a \sim (0.1-0.35)$. Therefore, at $z = h$, and following equation (11), parameter β^2 is proportional to $k^{-1}\phi_h(\zeta)(u_h/u*)$ and, consequently, β^2 is proportional to $(S_t^{-1}\ C_d^{-1/2})$ where S_t and C_d are the Stanton number and drag coefficient, respectively [*Brutsaert*, 1982; *Stull*, 1991]. In the roughness and inertial sublayers, from equation (12), parameter β^2 is proportional to S_t^{-1}. The Stanton number represents a heat transfer coefficient, so S_t^{-1} represents a resistance to the sensible heat transport. In general, during daylight hours the Stanton number and drag coefficient are higher than during night. That is, according to Figure 3, under unstable conditions, parameter β is smaller than under stable conditions because it represents a dimensionless aerodynamic resistance to the sensible heat flux.

[22] When measuring at the canopy top near-neutral conditions, combining the scale, $1/\tau \sim a\, u_h/h$, with equation (11), it is possible to derive the following relationship: $(k\pi)\beta^2 \sim 0.74\ h/b(\tau u*)^{-1}$. The stability function for heat is $\phi_h(\zeta) \sim 0.74$, the coefficient b is $b = z*/h$ which ranges from 1 to 3.5 [*Brutsaert*, 1982, Figure 3.1, and references therein; *Cellier and Brunet*, 1992] and an appropriate value for the parameter β following Figure 3 is $\beta \sim 0.5$ for a variety of canopies. If we take the zero plane displacement and surface roughness (z_0) heights as 2/3–0.67 and 0.12 times the canopy height [*Brutsaert*, 1982; *Wieringa*, 1993], respectively, a reasonable relationship between friction velocity and wind speed measured close to the canopy top would be as follows: $u* \sim ku_h/\ln[(z\text{-}d)/z_0] \sim u_h/3$, which is in accordance with measurements made by several authors (see Table 1, and for further details, also see *Raupach et al.* [1996, Table 1, and references therein]). This leads to the following relationship for estimating ramp frequency: $1/\tau = [b/3(k\pi)\beta^2/0.74]\ u_h/h \sim (0.11-0.33)\ u_h/h$. This relationship is compatible with the linear stability theory of *Raupach et al.* [1989] and also concurs with reported values determined for different canopies and from wind tunnel experiments. For further details, see *Raupach et al.* [1996, sect. 2.2], *Chen et al.* [1997a, Figure 13], and *Shaw et al.* [1995].

2.3. Explaining Parameter α

[23] Combining equation (3) with the corresponding equations (4) and (5), sensible heat flux can be expressed by

$$H = \begin{cases} \rho C_p (k\beta) u_* \phi_h^{-1}(\varsigma) A & \text{if } z > z^* \\ \rho C_p \dfrac{z^*}{z} (k\beta) u_* \phi_h^{-1}(\varsigma) A & \text{if } h \le z \le z^* \end{cases} \tag{13}$$

An expression for determining parameter α can therefore be derived by equating (1) and (13) and combining with equation (11). After rearranging terms, parameter α is given by

$$\alpha = \begin{cases} \left[\dfrac{k}{\pi}\dfrac{(z-d)}{z^2}\tau u_* \phi_h^{-1}(\varsigma)\right]^{1/2} & \text{if } (z-d) > z^* \\ \left[\dfrac{k}{\pi}\dfrac{z^*}{z^2}\tau u_* \phi_h^{-1}(\varsigma)\right]^{1/2} & \text{if } h \le (z-d) \le z^* \end{cases} \tag{14}$$

Castellvi et al. [2002] interpreted parameter (αz) as the mean eddy size responsible for renewal. Equation (14) therefore suggests that mean eddy size scales with the geometric mean of $(z\text{-}d)$ or z^* and $\phi_h^{-1}(\zeta)$ (τu_*), in the inertial and roughness sublayers, respectively.

[24] When measuring close to the canopy top, parameter α depends on the canopy structure through z*. Roughness layer depth may be scaled according to the mean spacing between plants in sparse vegetation, interrow spacing in orchards and canopy height for homogeneous vegetation [*Garratt*, 1980; *Brutsaert*, 1982; *Cellier*, 1986]. For tall and crown dense canopies when measuring at the canopy top, parameter α is close to 0.5, regardless the ramp model used and method applied to determine the ramp dimensions. Then, equation (14) should be able to qualitatively analyze the ratio, z*/h, for these canopies when measuring at the canopy top. Combining equation (14) with the relationship, $1/\tau \sim a\, u_h/h$, the expression obtained for, z^*/h, is the following: $z^*/h = (\alpha^2 \pi a/k)(u_h/u_*)\phi_h(\zeta)$. In Table 1 are shown z^*/h values obtained by the latter z^*/h expression for different homogeneous canopies at near-neutral conditions ($\phi_h(\zeta)$ was set to 0.74) based on measurements made by several authors [see *Raupach et al.*, 1996, Table 1, and references therein]. It is shown that most z^*/h values fall into the reported range, $z^*/h \sim (1, 3.5)$ [*Brutsaert*, 1982, Figure 3.1, and references therein; *Cellier and Brunet*, 1992].

[25] Equation (14) is able to explain the parameter α features described in section 2.1. Equation (14) shows that α values depend on measurement height and stability conditions. According to *Gao et al.* [1989], ramp duration is fairly constant with height. Therefore, when measuring in the roughness sublayer, the closer the measurement level is to the canopy top the greater the calibrated value for α. In the inertial sublayer, α decreases as measurement height increases. Equation (14) suggests that calibration of α for a given height and canopy is variable as it depends on stability conditions. Qualitatively analyzing the dependence

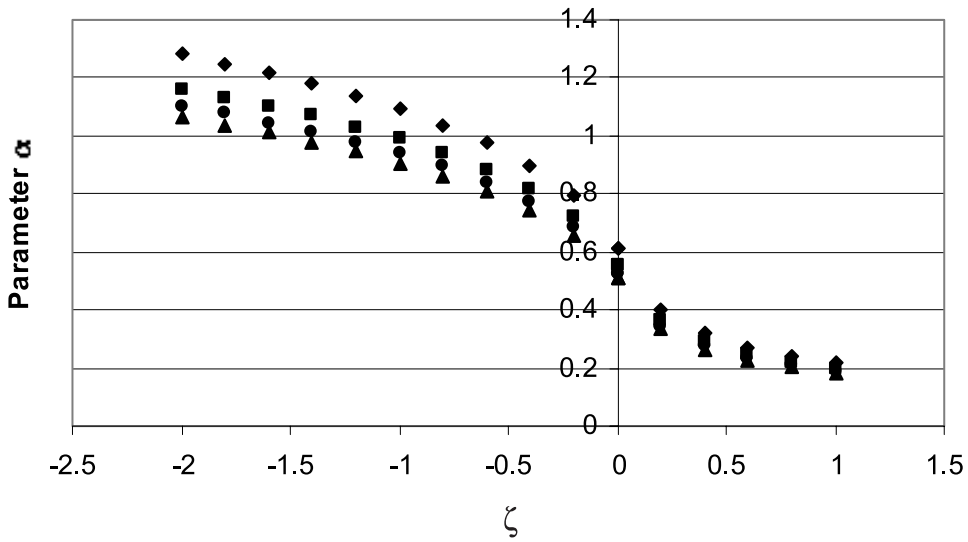

Figure 4. The parameter α, equation (15), stability parameter relationship for bare soil (diamonds), straw mulch with a measurement height in the roughness sublayer (squares) and at the top of the roughness sublayer (circles), and Douglas fir forest (triangles).

of parameter α on the stability conditions, as performed for parameter β in Figure 3, equation (14) is rewritten as follows:

$$\alpha = \begin{cases} \dfrac{(z-d)}{z}\left[\dfrac{k}{\pi}\dfrac{\phi_h^{-1}(\varsigma)}{\lambda}\right]^{1/2} & \text{if } (z-d) > z^* \\ \left[\dfrac{k}{\pi}\dfrac{z^*}{z}\dfrac{\phi_h^{-1}(\varsigma)}{\lambda}\right]^{1/2} & \text{if } h \le (z-d) \le z^* \end{cases} \quad (15)$$

It should be remembered that equation (15) is valid for a fixed measurement because parameter λ is height dependent. Figure 4 shows a qualitative analysis of α dependence on the stability parameter. It uses the same λ values corresponding to measurement heights for bare soil, straw mulch and Douglas fir forest, as used in Figure 3. The variables in equation (15) for the plots in Figure 4 were as follows: for bare soil, the zero-plane displacement was set to zero; for straw mulch and Douglas fir forest we assumed $z^* = 5/3h$; measurement levels above the canopy (z/h) were set to $z/h = 0.09/0.06 = 1.5$ and $z/h = 23/16.8 = 1.34$ for straw mulch and Douglas fir forest, respectively. Figure 4 also shows the dependence of α on the stability parameter when it is assumed that the measurement level for straw mulch is just at the top of the roughness sublayer ($z = z^*$), because for this canopy $z/h = 1.5$ is close to $z^*/h \sim 5/3$. Figure 4 shows the tendency for α to increase when buoyancy effects in the surface layer become more important, which indicates that the air parcel becomes uniformly heated, regardless of measurement height. Regardless of the surface, the α parameter tends to diminish to approximately 0.2 under very stable conditions. This trend confirms the findings shown by *Paw U et al.* [1995]: calibrated α values are lower under stable than unstable conditions. Figure 4 also shows that near-neutral conditions parameter α is close to 0.5 and for the following range of the stability parameter, $-0.25 \le \zeta \le 0.25$, the slopes of the four curves are steep with values of around -0.6. This indicates that mixing samples collected under both unstable and stable conditions may considerably distort the α calibration. Variations in parameter α with respect to the stability parameter can be interpreted as increases or decreases in mean vertical eddy size responsible for renewal as surface layers become respectively more unstable or stable. Thus air parcels in the inertial and roughness sublayers are renewed by eddies that vary in size under neutral, unstable and stable conditions thus confirming results from *Katul et al.* [1996].

[26] Overall, despite the use of a fixed measurement level above the canopy top, equation (14) exposes the limitations of using equation (1) with a calibrated parameter α to estimate sensible heat flux at sites with a wide ranging stability parameter. Air temperature and wind speed are required as input to determine the appropriate parameter α. The original attractiveness attributed to equation (1) for estimating sensible heat flux exclusively from air temperature measurements should therefore be generally questioned. Here, in section 4 is shown the variability of parameter α for half-hourly periods when measuring at a fixed height. This variability is a consequence of the shear stress through friction velocity and the strong dependence that $\phi_h(\zeta)^{-1/2}$ introduces into (14) with respect the stability parameter. However, although SR approaches may implement wind velocity, they are still interesting since SR can be used below the inertial sublayer.

2.4. Estimating Sensible Heat Flux

[27] A new SR approach for estimating sensible heat flux can be obtained by combining equations (1) and (14). It can also be obtained by combining equations (3) and (11), or equations (2), (11), (C5) and the scale $\varepsilon_t = A^2/(\tau\pi)$ (see Appendix C). The resulting expression is given by

$$H = \begin{cases} \rho C_p \left(\dfrac{k(z-d)}{\pi}\right)^{1/2} \tau^{-1/2} A \left(\phi_h^{-1}(\varsigma) u_*\right)^{1/2} & \text{if } (z-d) > z^* \\ \rho C_p \left(\dfrac{kz^*}{\pi}\right)^{1/2} \tau^{-1/2} A \left(\phi_h^{-1}(\varsigma) u_*\right)^{1/2} & \text{if } h \le (z-d) \le z^* \end{cases} . \quad (16)$$

From the invoked assumptions, equation (16) is valid when measurements are made over homogeneous canopies and

stationary conditions apply during the sampling period, (t-t_o), which is typically about half an hour, since net radiation does not generally change significantly over such a period. Equation (16) is exempt from calibration regardless of the stability conditions. Air temperature and wind speed measurements are needed because friction velocity and the stability parameter are required as input. Thus an iterative method can be used to solve for (16). The stability parameter and the third moment of the temperature structure function, $S^3_{(r)}$, have the same sign, see equation (A5). The selection of the stability function for heat in (6) is therefore known from the air temperature measurements for each sample. Apart from the ramp-amplitude, equation (16) depends on the square root of the input variables; $\rho C_p \sim 1215$ holds for a large range of climatic conditions. Using equation (16), the square root dependence reduces errors in the estimation of sensible heat flux, which arise from errors in the determination of the input variables. This is particularly useful when determining the ramp frequency, because it depends on the third power of the amplitude, see equation (A5). Minor errors in determining the ramp amplitude may lead to important errors in the ramp duration. The following may be typical sources of errors: measurements made over canopies with partial soil cover; sites with inadequate fetch where measurements are often made outside the adjusted inertial sublayer and estimation of roughness sublayer depth.

[28] Appendix A includes a set of equations used to determine the ramp dimensions for the ramp model illustrated in Figure 2b by applying a constant parameter γ (see averaged γ values for different surfaces in Table A1). This substantially reduces numerical complexity because the microfront period is estimated and thus makes it possible to measure air temperature at reasonable frequencies. This is convenient for field applications because it avoids problems resulting from storage, data processing and using fragile fine-wire thermocouples: the higher the sampling frequency, the thinner the thermocouple wire diameter required. Combining equations (16) and (A5), the expression for estimating sensible heat flux is given by

$$H = \begin{cases} \rho C_p \left(\frac{k(z-d)}{\pi}\right)^{1/2} \left(-\gamma^3 \frac{S^3_{(rx)}}{r_x}\right)^{1/2} A^{-1/2} \left(\phi_h^{-1}(\varsigma) u_*\right)^{1/2} & \text{if } (z-d) > z^* \\ \rho C_p \left(\frac{kz^*}{\pi}\right)^{1/2} \left(-\gamma^3 \frac{S^3_{(rx)}}{r_x}\right)^{1/2} A^{-1/2} \left(\phi_h^{-1}(\varsigma) u_*\right)^{1/2} & \text{if } h \le (z-d) \le z^* \end{cases} \quad (17)$$

Also, by combining equations (7), (16) and (A5) the sensible heat flux is given by

$$H = \begin{cases} \rho C_p \left(\frac{g}{T}\right)^{1/5} \frac{(k(z-d))^{4/5}}{\pi^{3/5}} \left(-\gamma^3 \frac{S^3_{(rx)}}{r_x}\right)^{3/5} A^{-3/5} \left(\frac{\phi_h^{-3}(\varsigma)}{-\varsigma}\right)^{1/5} & \text{if } (z-d) > z^* \\ \rho C_p \left(\frac{g}{T}\right)^{1/5} k^{4/5} \left(\frac{z^*}{\pi}\right)^{3/5} z^{1/5} \left(-\gamma^3 \frac{S^3_{(rx)}}{r_x}\right)^{3/5} A^{-3/5} \left(\frac{\phi_h^{-3}(\varsigma)}{-\varsigma}\right)^{1/5} & \text{if } h \le (z-d) \le z^* \end{cases} \quad (18)$$

[29] Overall, equations (17) and (18), although not strictly exempt from calibration due to parameter γ, may provide better estimates than equations (1) and (3) or (8) that use calibrated α and β values, respectively. Parameter γ is rather conservative: it varies less than 25% with respect to unity for very different canopies [*Chen et al.*, 1997a], which may provide reasonable estimates of α and β for individual samples when applying equation (A5) in equations (14) and (11), respectively. Equations (17) or (18) may therefore capture a greater part of the variance for a given sensible heat flux data set than approaches using calibrated α and β values.

[30] According to the parameters required to describe turbulence under very unstable conditions, sensible heat flux must be independent of the stability parameter. The function $(-\varsigma\phi_h^3(\varsigma))^{-1/5}$ in equation (18) can be approximately set to 2.4 for the stability range $-0.03 \le \varsigma \le -3$, with a relative error of less than 8.5%. Equation (18) for estimating sensible heat flux under unstable conditions therefore approaches the following expression,

$$H = \begin{cases} 2..4\rho C_p \left(\frac{g}{T}\right)^{1/5} \frac{[k(z-d)]^{4/5}}{\pi^{3/5}} \left(-\gamma^3 \frac{S^3_{(rx)}}{r_x}\right)^{3/5} A^{-3/5} & \text{if } (z-d) > z^* \\ 2..4\rho C_p \left(\frac{g}{T}\right)^{1/5} k^{4/5} \left(\frac{z^*}{\pi}\right)^{3/5} z^{1/5} \left(-\gamma^3 \frac{S^3_{(rx)}}{r_x}\right)^{3/5} A^{-3/5} & \text{if } h \le (z-d) \le z^* \end{cases} \quad (19)$$

The approach obtained is attractive. It holds under slightly unstable conditions, is valid in both the roughness and inertial sublayers, and only requires temperature data as input.

3. Materials and Methods

3.1. Materials

[31] Three different canopies were analyzed: grass, wheat and grapevines. The campaigns undertaken were as follows.

3.1.1. Grass

[32] A three-dimensional sonic anemometer (R.M.Young, 8100) was installed at a height of 1.5 m above 0.1 m high, alta fescue grass, in the middle of a 100 m square plot at the Campbell Tract Experimental Farm (University of California at Davis). Air temperature and three wind components were recorded at 10 Hz for twelve days in mid-August 2001. A set of 166 half-hourly samples was collected under unstable conditions and a further 261 under stable conditions. A one-dimensional sonic anemometer (CA27, CSI) was installed at the same plot for days 86, 87 and 88 of the year 1994 at a height of 0.6 m. Three fine-wire thermocouples were also installed at 0.6, 0.9, and 1.2 m above ground level. A one-dimensional sonic anemometer (CA27, CSI) was installed for days 213 and 214 of year 1995 at 0.7 m and three thermocouples were installed at 0.7, 1.0, and 1.3 m above ground level. For these five days, the sonic anemometer recorded sensible heat flux (determined using raw data at 10 Hz) and mean half-hourly wind speed was measured at 2 m. The fine-wire thermocouples were identical: 7.6×10^{-5} m diameter and air temperature was measured at 8 Hz. A total set of 151 half-hourly samples was collected under unstable conditions during this five-day period. Very few samples were collected under stable conditions because the experiment was carried out during daylight hours.

3.1.2. Wheat

[33] This experiment was conducted for two days during daylight hours in spring of 1994 at the research station of the Univ. of California at Davis. A one-dimensional sonic

anemometer (CA27, CSI) was installed at a height of 2 m and used to store half-hourly sensible heat fluxes using raw data at 10 Hz. Three (7.6×10^{-5} m diameter) thermocouples were installed at heights of 0.7, 1.0 and 1.3 m above the ground and used to record air temperature at 8 Hz. Mean half-hourly wind speeds were recorded at a height of 2 m. The canopy height was 0.7 m and the crop was dense and well irrigated. A total set of 43 half-hourly samples were collected under unstable conditions.

3.1.3. Grapevines

[34] This experiment was conducted at Napa Valley for two days in the summer of 1995, during daylight hours. A one-dimensional sonic anemometer (CA27, CSI) was installed at a height of 3 m, recording half-hourly sensible heat fluxes using raw data at 10 Hz. Four (7.6×10^{-5} m diameter) thermocouples were deployed at 2, 2.3, 2.6 and 2.9 m above the ground level recording air temperature at 8 Hz. Mean half-hourly wind speeds were recorded at a height of 3 m. The canopy features were the following; 2 m high, 65% ground cover, and the space between plants and interrows were 1.2 m and 2.7 m, respectively. A total set of 133 half-hourly samples was made under unstable conditions.

3.2. Methods

3.2.1. Determining Air Surface Layer and Canopy Parameters

[35] In campaigns conducted over grass in 1994 and 1995, wheat and grapevines the actual stability parameter was determined using the iterative method 1 described in Appendix D but implementing the actual sensible heat flux. In the case of the campaign over grass conducted in the summer of 2001, this was determined from the raw data (see method 2 in Appendix D). The ranges of the stability parameter determined in each campaign were as follows: (−0.59, −0.06) for 1994, (−0.64, −0.08) for 1995 and (−2.66, 1.92) for 2001 for grass; (−0.92, −0.14) and (−0.6, 0.00), for wheat and grapevines respectively. The fetch requirements, assuming a relationship of 1:100, were met for wheat and grapevines, but not for grass, where the measurement heights were located above the adjusted inertial sublayer. The height of the zero plane displacement was determined as, $d = 2/3\ h$, with h as the canopy height. The roughness sublayer depth for wheat was estimated as, $z^* = h + 2\ (h\text{-}d)$, following *Sellers et al.* [1986]. For grapevines, the mean interrow spacing was taken as z*, *Garratt* [1980]. As an approximation of parameter γ, this was set to $\gamma = 1.1$ for each measurement height and canopy and the von Kármán constant was set to 0.35 in accordance with equation (6).

[36] The ramp amplitude was determined by averaging the solutions to (A2) for three different time lags close to the ramp peak, r_x. Following *Chen et al.* [1997a], very minor errors are obtained if the correct time lag tends to err to the left of the ramp peak as shown in Figure 2b, $r > r_x$. Air temperature was generally recorded at suitable frequencies (see Table A1). An exception was a subset when measuring under near-neutral conditions. For some samples the sign of the third moment of the temperature structure function was not consistent with the sign of actual sensible heat flux. These cases, 86 samples in total with 64 taken over grass, were removed to avoid distorting the results and obstructing the main purpose of this paper. In these cases, higher measurement frequencies were required to determine the correct ramp dimensions. Parameter β was determined using equation (11) because a very high frequency sampling rate is needed to determine the microfront period required to determine the portion p in (C3), whose differences may be negligible.

3.2.2. Flux Variance Method for Comparing Sensible Heat Flux Estimates

[37] The equation based on temperature variance [*Tillman*, 1972] was analyzed with the objective of comparing the performance of equations (17) or (18) and (19). This is a well-established equation for estimating the sensible heat flux that has been the subject of intensive research over the last decade, though mainly under unstable conditions [*Kader and Yaglom*, 1990; *Weaver*, 1990; *Lloyd et al.*, 1991; *Padro*, 1993; *Albertson et al.*, 1995; *Katul et al.*, 1996]. *Tillman* [1972] proposed

$$H = \begin{cases} \rho C_p \left(\frac{\sigma_T}{0.95}\right)^{3/2} \left(\frac{kg(z-d)}{T}\right)^{1/2} \left(\frac{0.05-\varsigma}{-\varsigma}\right)^{1/2} & \varsigma < 0 \\ -\rho C_p \left(\frac{\sigma_T}{C}\right)^{3/2} \left(\frac{kg(z-d)}{T}\varsigma\right)^{1/2} & \varsigma \le 0 \end{cases} \tag{20}$$

Where σ_T is the air temperature standard deviation measured at high frequency and C is an ill-defined constant. Several studies have shown that it ranges from −1.8 to −2.5 and that site-specific calibration is recommended [*Stull*, 1991; *DeBruin et al.*, 1993; *Wesson et al.*, 2001].

[38] Although equation (20) was valid for the inertial sublayer, it was also applied when measurements were made in the roughness sublayer. This was done to demonstrate different performances when similarity requirements were not well accomplished at the site of interest. Calibration of equation (20) is recommended when measuring close to the roughness sublayer or over nonuniform terrain, and when sensible heat fluxes are small. However, here it will be assumed that this is not possible, in order to allow comparison with (17). As mentioned above, parameter γ was set to 1.1 and equation (17) is therefore exempt from calibration. Consequently, equation (20) was assumed valid when measuring close to the canopy top. Under stable conditions, such as the case for grass in 2001, the computed stability parameter was used and the constant C was set to, $C = 2.0$ [*Stull*, 1991; *DeBruin et al.*, 1993]. The sensible heat flux from equation (20) was evaluated using the iterative procedure described in Appendix D, see method 1.

[39] According to *Albertson et al.* [1995], the free convection limit approach for the flux variance method still holds under slightly unstable conditions and can be expressed as

$$H = \left\{ \rho C_p \left(\frac{\sigma_T}{C_1}\right)^{3/2} \left(\frac{kg(z-d)}{T}\right)^{1/2} \varsigma \le -0.04 \right. \tag{21}$$

Where C_1 is a universal similarity constant that can be set to, $C_1 = 0.95$. This expression is very convenient when measuring within the inertial sublayer because sensible heat flux can be determined on line with actual data-loggers: the

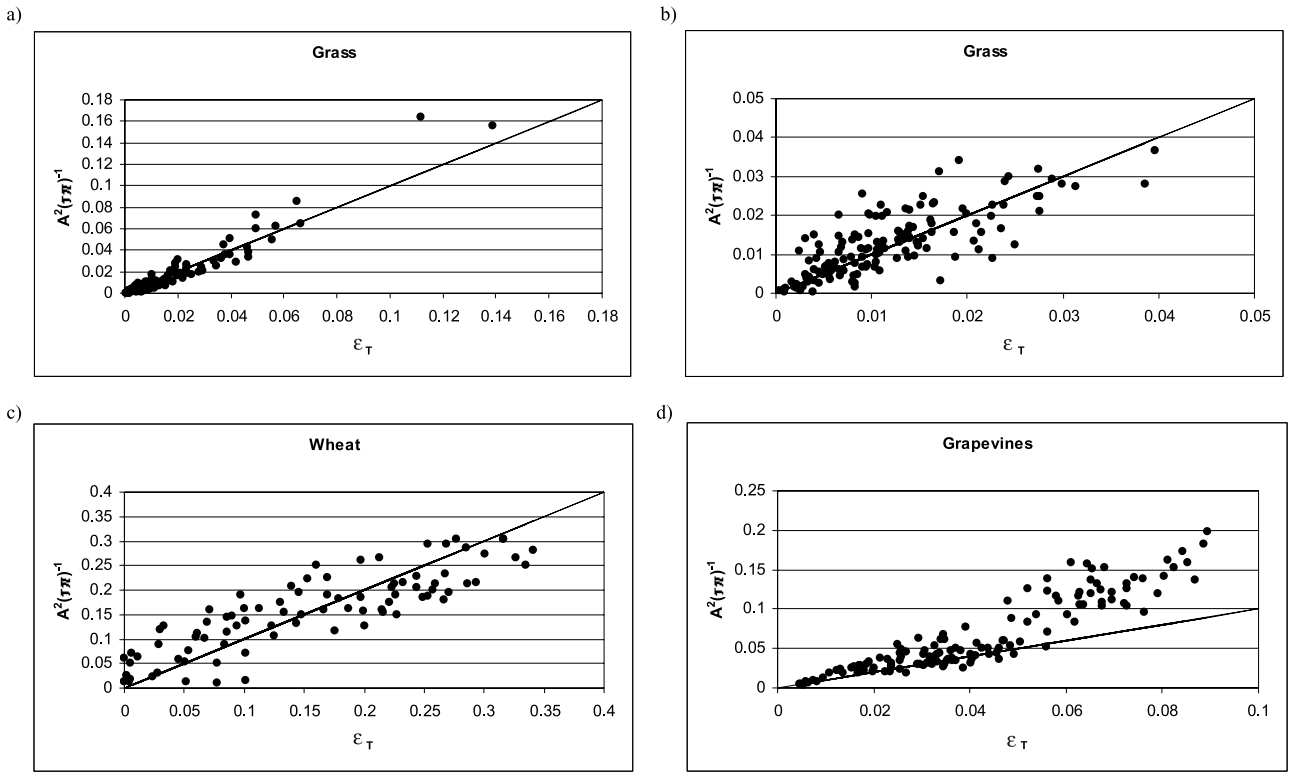

Figure 5. Dissipation rate of temperature variance ε_T versus $A^2/(\tau\pi)$. The 1:1 line is also shown for comparison. Grass (0.1 m tall) (a) for all samples collected at z = 0.6, 0.7, 0.9, and 1.00 m and (b) for all samples collected at z = 1.5 m. (c) Wheat (0.7 m tall). (d) Grapevines (2.0 m tall).

iteration method is not required. Therefore it is comparable to equation (19).

4. Results

4.1. Parameters β and α

4.1.1. Scaling the Dissipation Rate of Temperature Variance

[40] The alternative route proposed in Appendix C for describing parameter β, equation (11), assumed proportionality between the dissipation rate of temperature variance, ε_T, and the square of the ramp amplitude multiplied by the ramp frequency, $\varepsilon_T = A^2/(\tau\pi)$. This requires experimental evidence, since ε_T, A and τ must all be determined.

[41] The dissipation rate of temperature variance was obtained as described in Appendix D. According to the available data, method 1 was used for the experiments over grass conducted in 1994 and 1995. Figure 5a shows ε_T versus $A^2/(\tau\pi)$ corresponding to measurement levels; z = 0.6, 0.7, 0.9 and 1.00 m, in order to ensure as much as possible similarity theory hypotheses due to fetch requirements. The 1:1 line was also introduced to aid visual comparison. The slope obtained from a linear fitting through the origin and determination coefficient is shown in Table 2. They were 1.08 and 0.91, respectively. This excellent agreement suggests that the assumptions made when deriving (14) in section 2.2 were reliable.

[42] However, there remains the important question of what happens when similarity assumptions are not fully met. For the experiment carried out over grass in year 2001, in which the measurement level was well-above the surface adjusted layer according to the fetch requirements, the dissipation rate of temperature variance was obtained following the method 2, as described in Appendix D. Equation (D7) is a very stringent test of the inertial subrange scaling, but it is also straightforward, because it avoids the need to first determine the dissipation rate of turbulent kinetic energy, which is required when using spectral density analysis or second-order structure functions. The dissipation rate of temperature variance was determined from (D7) when turbulence intensity was less than 30%, and when at least five spatial lags in the flow direction, x, were obtained in the range, 0.3 m $\leq x \leq$ 0.8 m (see Appendix D), and gave a determination coefficient that was greater than 0.85. These constraints were imposed in order to accurately establish the inertial subrange scale [*Kiely et al.*, 1996]. A total of 151 samples were obtained under unstable conditions.

[43] As only mean wind velocity and temperature at high frequency were acquired in the other experiments over

Table 2. Slope (a), Obtained From Linear Fitting Through the Origin, and Determination Coefficient r^2, Corresponding to the Relationship $\varepsilon_T = A^2/(\tau\pi)$[a]

Canopy	a	r^2	Measurements Made
Grass	1.08	0.91	at z = 0.6, 0.7, 0.9 and 1.0 m
Grass	0.99	0.67	at z = 1.5 m
Wheat	0.92	0.64	in roughness sublayer
Grapevines	1.64	0.81	in roughness sublayer

[a]The results shown correspond to all the measurements made and indicate the height or sublayer for which the temperature data were acquired. See text.

Table 3. Actual Mean and Standard Deviation (σ) of Parameters β and α[a]

		Actual		Equation (11)		Actual		Equation (14)		Equation (14)	
Crop	z, m	β	σ_β	β	σ_β	α	σ_α	α	σ_α	Slope	RMSE
Grass	0.6	0.28	0.05	0.27	0.07	0.67	0.26	0.77	0.20	1.11	0.29
Grass	0.7	0.25	0.03	0.27	0.03	0.84	0.33	0.79	0.37	0.94	0.11
Grass	0.9	0.26	0.05	0.27	0.07	0.59	0.22	0.70	0.34	1.18	0.26
Grass	1.0	0.26	0.04	0.27	0.07	0.89	0.37	0.79	0.37	1.12	0.20
Grass	1.2	0.27	0.04	0.28	0.04	0.56	0.25	0.66	0.26	1.25	0.33
Grass	1.3	0.24	0.16	0.25	0.12	0.43	0.34	0.53	0.34	1.21	0.18
Grass	1.5	0.25	0.07	0.27	0.06	0.53	0.33	0.59	0.31	1.14	0.16
Grass	1.5[s]	0.82	0.27	0.75	0.22	0.21	0.08	0.23	0.06	0.76	0.08
Wheat	0.7	0.27	0.01	0.26	0.01	0.95	0.19	0.95	0.10	1.06	0.13
Wheat	1.0	0.25	0.01	0.25	0.01	0.74	0.19	0.72	0.12	1.00	0.26
Wheat	1.3	0.25	0.01	0.25	0.02	0.65	0.14	0.62	0.10	0.96	0.07
Grapevines	2.0	0.27	0.05	0.28	0.04	0.76	0.12	0.73	0.14	1.09	0.11
Grapevines	2.3	0.26	0.04	0.25	0.03	0.68	0.13	0.72	0.12	1.05	0.09
Grapevines	2.6	0.25	0.02	0.25	0.02	0.66	0.14	0.66	0.10	1.00	0.08
Grapevines	2.9	0.24	0.02	0.25	0.03	0.57	0.10	0.58	0.08	1.01	0.07

[a]Mean and standard deviations of parameters β and α determined for all levels by equations (11) and (14), respectively. Slope of estimated parameter α from equation (14) versus actual value obtained from a linear fit through the origin and root-mean-square error (RMSE). The superscript *s* denotes stable conditions.

wheat and grapes (all measurement levels were close to the canopy top), the dissipation rate of temperature variance was obtained as described in Appendix D, following method 1. It was assumed that all similarity constants and relationships still held when measuring close to the canopy top. Figures 5b, 5c, and 5d respectively show performance for experiments involving grass 2001, wheat and grapevines. All measurement levels are included in Figures 5c and 5d, and it is shown that a high correlation was also obtained for these experiments. The respective slopes obtained from a linear fitting through the origin and determination coefficients are shown in Table 2. The slopes obtained for the experiments conducted over grass and wheat were close to one, but the slope for grapevines differed from unity. For grapevines, the slopes and determination coefficients obtained for each measurement height were respectively: 1.87 and 0.82 at z = 2 m, 1.67 and 0.825 at z = 2.3 m, 1.62 and 0.85 at z = 2.6 m and 1.38 and 0.85 at z = 2.9 m. The slope tended to diminish when measurement height increases indicating that some of the 1:1 line departures could probably be attributed to the performance of similarity relationships close to the canopy top in the case of grapevines. These relationships appeared to be robust when the canopy was homogeneous, as in the grass and wheat experiments. The high correlation obtained could indicate that sensible heat flux estimates based on equations (11) or (14) should also correlate well with actual sensible heat flux. Performance when estimating sensible heat fluxes will be analyzed next. On the basis of the performance shown in Figures 5a, 5b, 5c, and 5d and assuming that the production and dissipation rates for temperature variance are similar ($\Phi_h(\zeta) \approx \Phi\varepsilon_T(\zeta)$, equation (D5), and for further details see *Kiely et al.* [1996]), equation (16) can also be considered a dissipation temperature- SR based equation for estimating sensible heat flux.

4.1.2. Estimating Parameters β and α

[44] The parameters β and α were determined for each half-hour sample from equations (13) and (1) using the actual sensible heat flux. These are referred to as the actual β and α parameters. Table 3 shows the resulting statistics determined for each crop and for all measurement heights; the actual means and standard deviations of parameters β and α; the means and standard deviations of parameters β and α as determined by equations (11) and (14), respectively; the slope corresponding to the estimated, equation (14), versus actual parameter α linear fit through the origin and the root-mean-square error (RMSE).

[45] Table 3 shows that whatever the measurement level and canopy type, the averaged actual and estimated values for parameter β were very similar. Equation (11) was also able to explain the standard deviation. The good estimates obtained over grapevines indicate that the mean interrow spacing for estimating roughness sublayer depth was reliable. For field applications, the value $\beta \sim (0.25–0.28)$ could therefore be recommended under unstable conditions, regardless of the measurement height and natural surface. This was because the standard deviations were very low, which indicated that parameter β was rather conservative, as was shown in Figure 3.

[46] In general, Table 3 also shows that the averaged actual parameter α and the value determined from (14) were both reasonably similar for each measurement height and canopy. Actual standard deviations and those determined by (14) were also generally very similar. The actual standard deviations between canopies were rather different. The standard deviations of the stability parameter for grass, wheat and grapevines were 0.46, 0.16 and 0.07, respectively. This indicated considerable dependency on the stability conditions. This is qualitatively inferred in Figure 4. Table 3 highlights the tendency for parameter α to diminish as measurement height increases in each campaign. Note that for campaigns over grass in 1994 and 1995, the levels were separated by 0.1 m and the differences between averaged and calibrated α values at similar levels were greater than between levels separated by 0.3 m corresponding to each campaign. In these two campaigns the ranges for the stability parameter were similar, but not the corresponding standard deviations. For campaigns over grass under unstable conditions in 1994 and 2001, ranges for the stability parameter were substantially different and

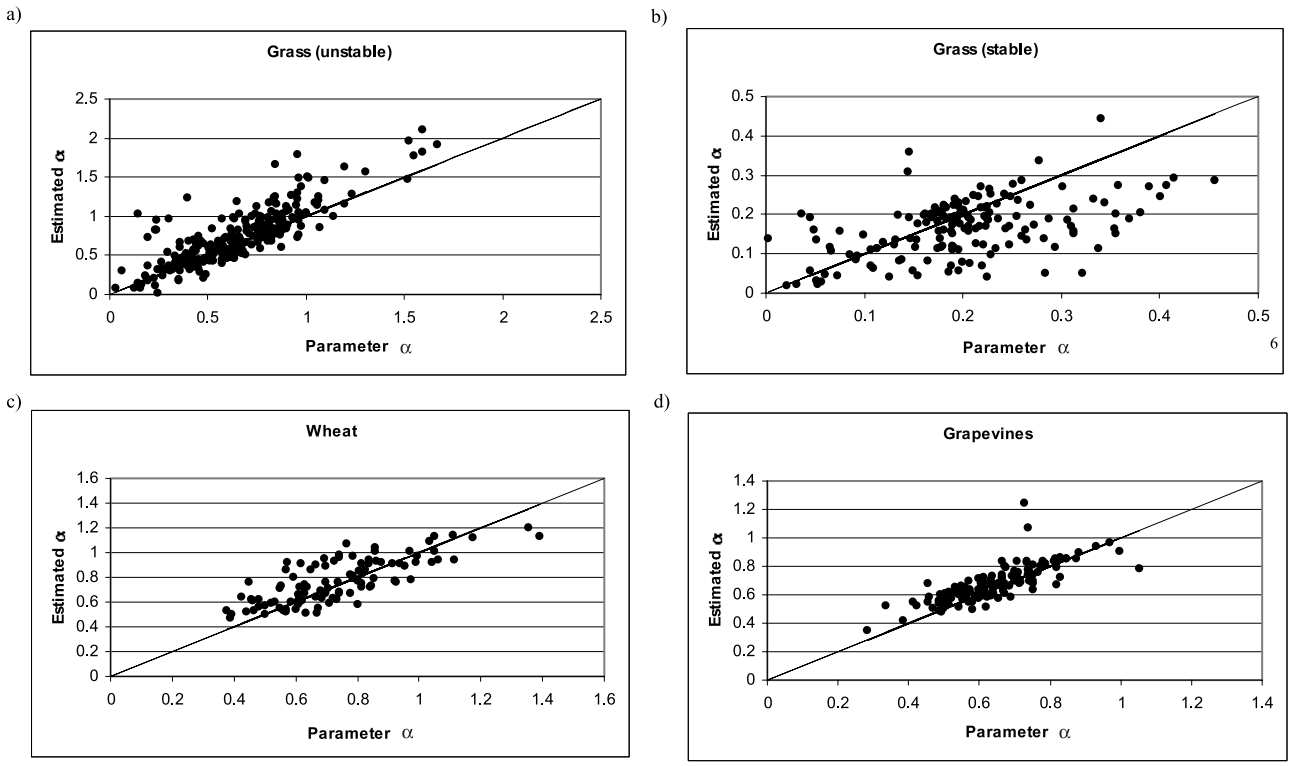

Figure 6. Estimated parameter α, equation (14), versus the α value determined after isolation in equation (1) using actual sensible heat flux. For grass under (a) unstable conditions and (b) stable conditions, (c) wheat, and (d) grapevines. The 1:1 line was introduced for comparison.

both averaged and calibrated α values were lower at the 1.3 m level in 1994 than those obtained at the 1.5 m level in 2001. This indicated the influence of stability conditions despite differences between the measurement heights. These results indicate the limitations of equation (1) for estimating sensible heat flux using a calibrated parameter α. Some differences may be attributed to the fact that thermocouple characteristics were different for the 1994 and 2001 campaigns, but those used for 1994 and 1995 had same characteristics.

[47] For a better sense of scatter, Figures 6a and 6b show parameter α determined from equation (14) over grass under unstable and stable conditions, respectively, versus the actual α value for the entire data set. Figures 6c and 6d also show parameter α determined over wheat and grapevines, respectively, for the whole data set. From these figures it can be seen that the performance of equation (14) was reasonable over grass and excellent for wheat and grapevines, regardless of measurement height. For better comparison, 1:1 lines were included in the corresponding figures. Table 3 presents the slopes obtained by a linear fit forced through the origin of equation (14) to show departures from the 1:1 line and the root mean square error, for each height. For the entire data set, the slopes obtained were close to unity, with low root mean square errors for wheat and grapevines. For grass, equation (14) overestimated parameter α under unstable conditions and underestimated it under stable conditions, by 14.5% and 25%, respectively.

[48] It is worthy to recall that the performances of equations (11) and (14) were good for all canopies when using a fixed parameter γ (γ = 1.1). This is crucial for obtaining a reliable approach for estimating sensible heat flux exempt from calibration.

4.2. Estimating Sensible Heat Flux

[49] Performance in estimating sensible heat flux was analyzed by a linear fit through the origin: the slope, determination coefficient, and the root mean square error were determined for equations (1), (13), (17), (19), (20) and (21) versus actual sensible heat flux (see Table 4). The results obtained for grass corresponding to the 1.5 m measurement height are shown separately for unstable and stable conditions.

[50] Sensible heat flux estimates involving equation (17) produced results that were generally superior to those obtained from equations (1) and (13) using specific-level calibration of parameters α and β, respectively (see Table 4). Taking parameter β as a constant to be calibrated, sensible heat flux estimates obtained from equations (8) and (13) are the same. Equation (17) is therefore superior to that proposed by *Castellví et al.* [2002]. As shown in Table 4, equation (13) generally performed better than equation (1); the determination coefficients were closer to unity and had lower root mean square errors, regardless of canopy and measurement heights. However, using equation (17) root mean square errors were substantially improved. This was because the α or β parameter was estimated for each half hour sample in (17). This resulted in slopes that were very close to unity; consequently equation (17) was able to capture more of the variance. This can be inferred from the generalized increase in the determination coefficient,

Table 4. Calibrated α and β Parameter for Equations (1) and (13), Respectively, and Slope From a Linear Fit Through the Origin for All Levels Corresponding to Equations (17), (19), (20), and (21) When Estimating Actual Sensible Heat Flux[a]

		Calibration		Slope				r^2				RMSE, W m^{-2}					
Crop	z, m	(1)	(13)	(17)	(19)	(20)	(21)	(1)	(13)	(17)	(19)	(20)	(21)	(1)	(13)	(17)	(19)	(20)	(20)[ac]	(21)
Grass	0.6	0.62	0.25	0.96	0.83	1.12	0.80	0.74	0.77	0.97	0.81	0.85	0.73	5.7	16.5	5.3	15.3	11.85		21.9
Grass	0.7	0.78	0.25	0.97	1.10	1.04	0.81	0.89	0.95	0.96	0.92	0.98	0.92	10.4	3.5	3.1	5.2	1.3		5.9
Grass	0.9	0.64	0.25	1.00	1.00	1.03	0.77	0.85	0.84	0.98	0.83	0.87	0.72	29.6	17.0	4.9	12.7	14.1		17.8
Grass	1.0	0.69	0.24	0.99	1.09	1.00	0.85	0.78	0.93	0.93	0.88	0.49	0.48	14.1	4.0	4.2	9.2	4.1		6.8
Grass	1.2	0.55	0.25	1.02	1.03	1.02	0.81	0.78	0.83	0.95	0.78	0.80	0.73	25.7	15.2	7.3	15.7	15.7		17.5
Grass	1.3	0.45	0.22	1.21	1.27	0.99	0.86	0.04	0.93	0.88	0.77	0.82	0.77	24.4	6.2	4.2	7.7	4.4		5.9
Grass	1.5	0.67	0.25	0.99	1.12	1.15	1.04	0.58	0.90	0.83	0.64	0.65	0.72	25.8	10.0	12.9	15.8	17.3		13.2
Grass	1.5[s]	0.29	0.87	1.03		—[b]		0.44	0.80	0.85		—[b]		6.0	7.6	3.9		29.5		
Wheat	0.7	1.01	0.27	1.12	1.01	1.63	1.50	0.55	0.70	0.74	0.66	0.59	0.68	84.6	64.7	58.7	47.5	188.3	54.5	144.7
Wheat	1.0	0.80	0.24	1.05	0.96	1.67	1.55	0.66	0.63	0.77	0.73	0.39	0.50	52.0	58.7	45.7	42.7	214.6	73.8	169.7
Wheat	1.3	0.70	0.25	1.01	0.92	1.52	1.40	0.44	0.62	0.76	0.78	0.35	0.40	81.2	65.3	42.5	45.5	181.3	76.2	141.8
Grapevines	2.0	0.77	0.25	0.96	1.01	1.27	0.68	0.85	0.84	0.95	0.83	0.74	0.13	41.1	39.6	17.8	26.7	79.8	43.3	82.1
Grapevines	2.3	0.69	0.25	0.94	1.00	1.60	0.85	0.86	0.85	0.94	0.85	0.83	0.31	40.0	37.0	22.45	26.8	143.4	42.0	63.9
Grapevines	2.6	0.62	0.24	0.90	0.96	1.63	0.87	0.83	0.84	0.94	0.87	0.84	0.24	33.0	36.6	28.5	24.5	145.1	37.8	65.8
Grapevines	2.9	0.56	0.24	0.91	0.99	1.75	0.94	0.74	0.85	0.94	0.87	0.86	0.30	36.5	36.0	26.3	25.7	167.0	45.8	64.3

[a]Determination coefficient r^2, corresponding to the linear regression, and the RMSE are also determined. The superscript *s* denotes stable conditions, and superscript *ac* denotes after calibration. See text.
[b]Equation (20) was unable to capture the variability of the actual sensible heat flux.

which could be interpreted as the portion of the variance that corresponds to the estimated sensible heat flux attributed to the variance of the actual sensible heat flux. Equation (17) performed well for all canopies, levels and stability conditions. The root mean square errors obtained with (17) were of a similar magnitude to errors typically associated with eddy covariance systems [*Foken and Wichura*, 1996].

[51] Figures 7a, 7b, and 7c show equation (17) estimates versus actual sensible heat flux over grass, wheat and grapevines, respectively, for the entire data set. It is particularly interesting to note that equation (17) was able to provide good estimations under nonideal conditions mainly for grapevines, where part of the sensible heat flux measured came from the soil. The slopes obtained by equation (17) over grapevines were close to unity, indicating that part of the bias shown in Figure 5d may be attributed to the performance in such field conditions of the similarity relationships involved in the method for determining the dissipation rate of temperature variance.

[52] It should be noted that equation (19) performed similarly (and even better in some cases) to (17) for lower levels in experiments over grass, wheat and grapevines. This suggests that under unstable conditions, it may also be possible to accurately estimate sensible heat flux using temperature measurements as input when measuring close to the canopy top. In general, the results shown in Table 4 indicate that when measuring in the inertial sublayer, equation (19) performs slightly better than (1) and is comparable to (13), while it is superior to equations (1) and (13) when measuring in the roughness sublayer.

[53] When measuring well above the canopy (experiments over grass), good estimates were also obtained using the flux variance method under unstable conditions; equation (20). Estimates obtained from (20) under unstable conditions were slightly better than (1) and comparable to those from equations (13), (17) and (19). The slope and determination coefficient corresponding to the linear fit through the origin for the experiment over grass at a measurement height of z = 1.5 m under stable conditions are not shown, because the covariance between estimated and actual sensible heat fluxes was negative; -61.7 W^2 m^{-4}. This indicates that there were large errors. The root mean square error obtained was 29.5 W m^{-2} and 56% of the samples had sensible heat fluxes of less than 29.5 W m^{-2}. An explanation for this poor performance lies in the fact that the measurement height was located above the surface adjusted inertial sublayer and, as a result, the temperature variance was contaminated by the heat sources of their surroundings.

[54] When measuring close to the canopy top over wheat and grapes, the determination coefficients for equation (20) were high. This indicated the need for prior calibration of (D3) in order to reduce the RMSE for sensible heat flux. This performance was in accordance with *Weaver* [1990] and *Katul et al.* [1995]. After direct calibration of equation (20) with the actual sensible heat flux, the root mean square errors obtained from (20) were similar to those obtained from equations (1) and (13) and greater than those obtained from equations (17) and (19). The new RMSE obtained are shown in Table 4. Equations (17) and (19) therefore demonstrated clearly superior performance.

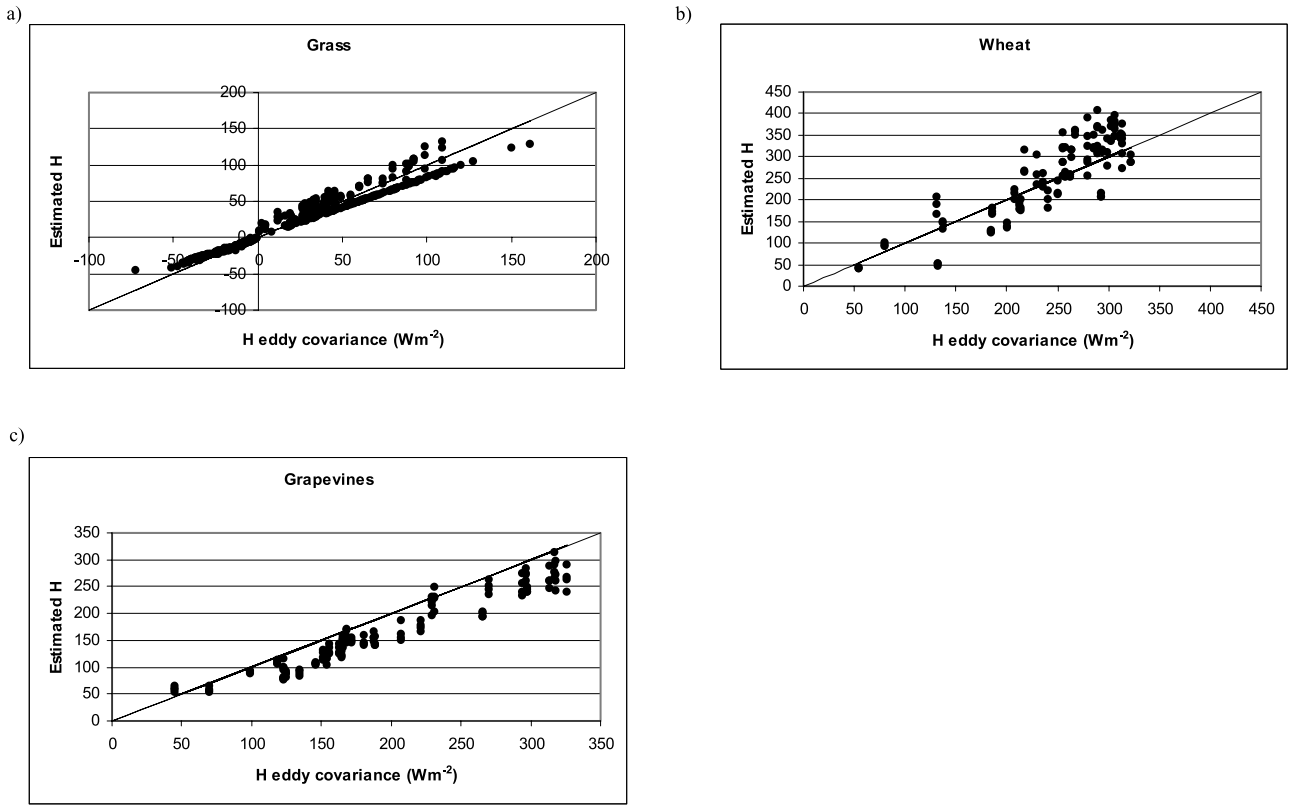

Figure 7. Estimates from equation (17) versus actual sensible heat flux (H) in W m^{-2} corresponding to all data sets. (a) Grass, (b) wheat, and (c) grapevines. The 1:1 line was introduced for comparison.

[55] Sensible heat estimates obtained by the flux variance method under unstable conditions following equation (21) were also good for the grass experiments. When measuring close to the canopy top, it is interesting to note that over wheat (uniform canopy) the performance was similar to that obtained using equation (20). Following prior calibration of the constant C_1 in order to correct the bias, performance was generally as good as that obtained from equation (20). However, over grapevines (nonuniform canopy), equation (21) was unable to capture reasonable percentages of sensible heat flux variability at any measurement level. That was not the case with equation (20). For the higher measurement levels, the slopes were reasonably close to unity, indicating that equation (21) was not biased. This performance therefore suggests that equation (20) could be more reliable than equation (21) for field purposes after calibration when the similarity assumptions are not fully met. Equations (19) and (21) are directly comparable since they require the same input data and cover a similar atmospheric stability range ($\zeta \leq -0.04$). Table 4 shows that the two equations performed similarly over grass, however, when measuring close to the canopy top, equation (19) was clearly superior and consequently appears advantageous when measurements of sensible heat flux are needed at canopies with difficult access or when fetch requirements are limited.

[56] Overall, the good performance of equations (11) and (14) led to equation (17) proving clearly superior and its free convection limit expression, equation (19), was comparable in the inertial sublayer and superior when measuring in the roughness sublayer with respect equations (1), (13), (20) and (21). In practice, equations (17) and (19) may be considered either exempt from calibration or rather conservative, regardless of the stability conditions and measurement height above a canopy. They performed well under nonideal field conditions. Surface renewal analysis may be inconsistent with the sign of actual sensible heat flux when measuring at a reasonable frequency under near-neutral conditions. The errors associated with these samples often fall within the measurement error. Under neutral conditions, ramp amplitude and frequency are small. The flux variance method performed well under unstable conditions when measurements were taken in the fully adjusted surface layer. After calibration, the flux variance method may also give good estimates when the assumed similarity constraints are not fully met. Equation (20) may be more suitable than equation (21) particularly when the canopy is nonuniform. Here, the flux variance method performed poorly under stable conditions. Under unstable conditions, and when measuring in the inertial sublayer, equation (21) is attractive because sensible heat flux estimates can be recorded on line. However, assumptions and measurements must be implemented to identify unstable atmospheric conditions. For example, *Wesson et al.* [2001] assumed unstable conditions when net radiation was positive. The determination of the sign of the ramp amplitude may be an alternative method for determining when equation (21) can be used. However, as this method requires the calculation of the third moment structure function, equation (19) can be implemented when similarity assumptions

are not fully met in the field, because it proved superior to the flux variance method.

5. Concluding Remarks

[57] Equation (16) constitutes a new equation for estimating sensible heat flux. It combines surface renewal analysis and similarity theory and is exempt from calibration. It was derived as a consequence of understanding parameter β in equation (2). It also led to (1) a new scale for the dissipation rate of the temperature variance, $\varepsilon_T = A^2/(\tau\pi)$ and (2) a better understanding of parameter α, which is crucial for estimating sensible heat flux using surface renewal analysis, equation (1). Limited performance for equation (1) is described when the calibration of parameter α is assumed for a given level. This depends on the canopy structure, shear stress and stability conditions. A problem therefore arises when we need to estimate sensible heat flux using only air temperature measurements above the canopy top. Strong evidence was presented to suggest that parameter $\beta_1 = (k\beta) \sim 0.1$ [*Castellví et al.*, 2002] could, in practice, be universally assumed under unstable conditions.

[58] When equation (16) was used in the form of equation (17) or equation (18), it was very accurate and presented interesting field advantages. Equation (17) depends on an averaged parameter (γ). It was fixed to $\gamma = 1.1$ and provided good estimates of parameters α and β for each sample, canopy and measurement height. In practice, based on the good performance, equation (17) can therefore be considered exempt from calibration either in the roughness and inertial sublayers regardless of the atmospheric stability conditions. Equation (19) was obtained as a free convection limit for equation (17) or equation (18). It holds for slightly unstable atmospheric conditions and provided excellent estimates, particularly when measuring in the roughness sublayer.

[59] The flux variance method required calibration when measuring close to the canopy top and performed poorly under stable conditions. As with other methods that are exclusively based on similarity principles, equation (17) also requires wind speed and air temperature measurements, but it escapes the typical limitations introduced by fetch requirements and assumptions that identify the atmospheric stability conditions. The new method showed performed excellently over canopies and measurement heights under what were far from ideal field conditions. It can hence be concluded that equation (17), and its free convection limit approach, equation (19), represent advantageous alternatives for estimating sensible heat flux.

Appendix A: Determination of the Ramp Parameters

[60] As the two ramp models provide similar results when determining ramp amplitude [*Chen et al.*, 1997a], structure functions (equation (A1)) and analysis technique (equations (A2) to (A4)) from *Van Atta* [1977] were applied:

$$S^n_{(r)} = \frac{1}{m-j}\sum_{i=1+j}^{m}\left(T_i - T_{i-j}\right)^n \tag{A1}$$

where m is the number of data points in the 30-minute interval measured at frequency (f) in Hz, n is the power of the function, j is a sample lag between data points corresponding to a time lag ($r = j/f$), and T_i is the ith temperature sample. An estimate of the mean value for A is determined by solving (A2) for the real roots:

$$A^3 + pA + q = 0 \tag{A2}$$

where

$$p = 10S^2_{(r)} - \frac{S^5_{(r)}}{S^3_{(r)}} \tag{A3}$$

and

$$q = 10S^3_{(r)} \tag{A4}$$

According to *Chen et al.* [1997a], the relationship between the inverse ramp frequency (τ) and ramp amplitude according to Figure 2b is

$$\frac{A}{\tau^{1/3}} = -\gamma\left(\frac{S^3_{(r_x)}}{r_x}\right)^{1/3} \tag{A5}$$

The microfront period, L_f, is given by,

$$L_f = (\gamma/_2)^{1/2} r_x \tag{A6}$$

where r_x is the time lag r that maximizes $(S^3_{(r)}/r)$ and γ is a parameter that corrects for the difference between $A/\tau^{1/3}$ and the maximum value of $(S^3_{(r)}/r)^{1/3}$. Parameter γ varies by less than 25% with respect to unity, (0.9–1.2), for the range of canopies in Table A1. For bare soil and straw mulch, parameter γ mainly varies between (1 and 1.2), while for Douglas fir forest it mainly varies between (0.9 and 1.1). Table A1 shows mean values for parameters γ and r_x and suitable measurement frequencies (in Hz) for different canopies required to solve equation (A5) (i.e., to find the appropriate solution to equation (A5) for the majority of samples) [*Chen et al.*, 1997a, 1997b].

Table A1. Recommended Mean Values for γ and r_x and Sampling Frequencies for Different Canopies

Canopy and Height	γ, s	Sampling Frequency, Hz	r_x, s
Fir forest, 16.7 m	1.001	5	0.833
Straw mulch, 0.06 m	1.175	11	0.111
Bare soil	1.104	26	0.066

Appendix B: Derivation of Equation (10)

[61] The derivation presented below using fractional analysis is also given by *Wang and Bras* [1998]. For simplicity, a neutral initial condition was assumed with $T(z_0, t_0) = 0$ and $T(z_1, t_0) = 0$, vertical temperature gradient is zero at time t_0. The Laplace transform of temperature with respect to time is denoted here as $Tl_{(s)}$. Assuming a turbulent eddy diffusivity, K_h, constant over a period ($t - t_0$), the Laplace transform with respect to time in equation (9), leads to

$$s\ Tl_{(s)} = K_h\frac{\partial^2 Tl_{(s)}}{\partial^2 z} \tag{B1}$$

The general solution to the differential equation presented above is

$$Tl_{(s)} = A(s)e^{-z\sqrt{s/sK_h}} + B(s)e^{z\sqrt{s/K_h}} \tag{B2}$$

A realistic physical solution for the last equation requires $B(s) = 0$, as the trend for mean temperature versus height diminishes (a finite temperature value is needed when z_1 is large). The derivative of $Tl_{(s)}$ versus z is expressed as

$$\frac{\partial Tl_{(s)}}{\partial z} = -\sqrt{1/K_h}s\ Tl_{(z,s)}\sqrt{s^{-1}} \tag{B3}$$

The inverse of the Laplace transform, and the definition of convolution in (B3) lead to the expression:

$$\frac{\partial T_{(z,t)}}{\partial z} = -\frac{1}{\sqrt{\pi K_h}}\int_{t_0}^{t}\frac{\partial T_{(z,s)}}{\partial s}\frac{\partial s}{\sqrt{(t-s)}} \tag{B4}$$

However, for questions of convenience, the following equivalent expression for equation (B4) is used in the text:

$$\frac{\partial T_{(z,t)}}{\partial z} = \frac{2}{\sqrt{\pi K_h}}\int_{t_0}^{t}\frac{\partial T_{(z,s)}}{\partial s}d\left(\sqrt{(t-s)}\right) \tag{B5}$$

Appendix C: Derivation of Equation (11)

[62] The ramp event shown in Figure 2b better describes the SR abstraction and was used to solve equation (10). Under unstable conditions, dT/ds is constant and has values of A/L_r when the air parcel is heated during contact with surface heat sources and $-A/L_f$ during the renewal phase. Thus the solution for the integral in equation (10), when the integration is over a ramp event under unstable conditions, can be expressed as

$$\begin{aligned}\int_0^{\tau}\frac{\partial T_{(z,s)}}{\partial s}d\left(\sqrt{(t-s)}\right) &= \frac{A}{L_r}\int_0^{L_r}d\left(\sqrt{(L_r-s)}\right)\\ &+\left[-\frac{A}{L_f}\int_0^{\tau}d\left(\sqrt{(\tau-s)}\right)+\frac{A}{L_f}\int_0^{L_r}d\left(\sqrt{(L_r-s)}\right)\right]\\ &= \frac{-A}{L_r}\sqrt{L}+\frac{A}{L_f}\left(\sqrt{\tau}-\sqrt{L_r}\right)\end{aligned} \tag{C1}$$

Under stable conditions, equation (C1) has the opposite sign. According to Appendix B, integration must begin when the temperature gradient is zero, since initial neutral conditions are assumed at t_o. Note that integration in (C1) starts in the quiescent period. The quiescent period was neglected in Figure 2b for simplicity. During the quiescent period (see Figure 2a), net injections of sensible heat flux are assumed to be zero, since temperature remains constant over time.

[63] The fraction of the ramp duration corresponding to the heating period (or cooling period under stable conditions) is denoted as, p. Therefore $L_r = p\tau$, and $L_f = (1-p)\tau$. Consequently, the temperature gradient described in equation (10) after expressing equation (C1) in terms of p, can be approximated as follows:

$$\frac{\partial T_{(z,t)}}{\partial z} = \frac{2A}{\sqrt{\tau\pi K_h}}\left[\frac{1}{\sqrt{p}}-\frac{\left(1-\sqrt{p}\right)}{(1-p)}\right] \tag{C2}$$

Combining equations (2) and (C2), the parameter β can be expressed as

$$\beta = \begin{cases}\dfrac{2(z-d)}{\sqrt{\tau\pi K_h}}\left[\dfrac{1}{\sqrt{p}}-\dfrac{\left(1-\sqrt{p}\right)}{(1-p)}\right] & if\ (z-d) > z^*\\ \dfrac{2z}{\sqrt{\tau\pi K_h^*}}\left[\dfrac{1}{\sqrt{p}}-\dfrac{\left(1-\sqrt{p}\right)}{(1-p)}\right] & if\ h \le (z-d) \le z^*\end{cases} \tag{C3}$$

Where h denotes the canopy height. Following *Chen et al.* [1997a], typical values for the ratio L_f/τ are approximately; 0.025, 0.058 and 0.0038 for bare soil, (6.6 cm thick) straw mulch and (16.5 m high) Douglas fir forest, respectively. Therefore, for most natural surfaces the fraction p, expressed in percentage terms, ranges between 94% and 99.9%. Consequently, equation (C3) can be approximated by the following expression:

$$\beta \approx \begin{cases}\dfrac{(z-d)}{\sqrt{\tau\pi K_h}} & if\ (z-d) > z^*\\ \dfrac{z}{\sqrt{\tau\pi K_h^*}} & if\ h \le (z-d) \le z^*\end{cases} \tag{C4}$$

An alternative route for describing parameter β may be as follows: starting from a simplified temperature variance (V_t) budget equation form, see equation (C5) below [*Brutsaert*, 1982; *Stull*, 1991],

$$\left(H/\rho C_p\right)\delta T/\delta z \approx \varepsilon_T \tag{C5}$$

where ε_T, denotes the mean dissipation rate of 0.5 V_t. Equation (C5) holds under stationary and homogeneous conditions and when the flux divergence term can be neglected such as above a canopy. Combining equations (1), (2), and (C5), ε_T scales with A^2/τ. Therefore it follows that using the flux gradient relationship, ($H/\rho C_p = K_h\ \delta T/\delta z$), equation (C5) can be rewritten as follows:

$$K_h(\delta T/\delta z)^2 \propto A^2/\tau \tag{C6}$$

Combining equations (C6) and (2) the following general relationship is obtained:

$$\beta \propto \begin{cases}\dfrac{(z-d)}{\sqrt{\tau K_h}} & \text{if } (z-d) > z^*\\ \dfrac{z}{\sqrt{\tau K_h^*}} & \text{if } h \le (z-d) \le z^*\end{cases} \tag{C7}$$

Equation (C7) will be the same as (C4) if the proportion between ε_T and A^2/τ is π^{-1}. This requires experimental verification.

[64] Equation (C4) admits any constant value representative of the turbulent eddy diffusivity during the integration period. Here, it is assumed that equations (4) and (5) are appropriate. Therefore, combining equations (4), (5) and (C4), it is possible to determine a representative parameter β

value that is valid for each sample period (typically half an hour) as follows:

$$\beta = \begin{cases} \left[\dfrac{(z-d)}{k\pi}\dfrac{\phi_h(\zeta)}{\tau u_*}\right]^{1/2} & \text{if } (z-d) > z^* \\ \left[\dfrac{z^2}{k\pi z^*}\dfrac{\phi_h(\zeta)}{\tau u_*}\right]^{1/2} & \text{if } h \le (z-d) \le z^* \end{cases} \quad \text{(C8)}$$

Appendix D: Determination of Sensible Heat Flux and Dissipation Rate of Temperature Variance

[65] The method used for obtaining sensible heat flux estimates from equations (8), (13), (17) and (20), and the dissipation rate of temperature variance, ε_T, depends on the measurements acquired in each campaign. A description is provided when high-frequency temperature measurements are available and when either the mean wind velocity for a specific reference height or the velocity fluctuations is also acquired. For further details and other alternative methods, see *Brutsaert* [1982], *Stull* [1991], *DeBruin et al.* [1993], *Kaimal and Finnigan* [1994], *Kiely et al.* [1996], and *Hsieh and Katul* [1996].

D1. Method 1: Mean Wind Velocity at a Reference Height and High-Frequency Temperature Are Available

D1.1. Sensible Heat Flux

[66] The following iterative method can be implemented. A first approximation for the friction velocity, u_*, is determined using equations (D1) and (D2), assuming neutral conditions for the actual surface layer,

$$u_* = \frac{k u_r}{\ln \frac{(z_r - d)}{z_0}} - \Psi_m \quad \text{(D1)}$$

where u_r is the wind speed at reference height z_r; d and z_o are the zero plane displacement and the surface roughness height, which can be estimated for uniform canopies as 2/3h and 0.12h, respectively, with h as the canopy top [*Wieringa*, 1993]. Ψ_m is the diabatic profile function for momentum:

$$\Psi_m = \begin{cases} 2\ln(0.5(1+x)) + \ln\left(0.5\left(1+x^2\right)\right) - 2\arctan(x) + 0.5\pi & \zeta \le 0 \\ -4.7\zeta & \zeta > 0 \end{cases} \quad \text{(D2)}$$

where $x = (1-16\zeta)^{1/4}$. This gives a rough approximation of the actual friction velocity and provides the first approximation for sensible heat flux, (8), (13), (17), and subsequently for L_o, (7), and the stability parameter. The process is iterated until convergence is achieved.

[67] The sensible heat flux derived from equation (20) was evaluated through the temperature scale, T_*, defined as, $T_* = H(\rho C_p u_*)^{-1}$, which can be determined using the following similarity relationship [*Tillman*, 1972]:

$$T_* = \begin{cases} \sigma_T 0.95(0.05 - \varsigma)^{-1/3} & \varsigma < 0 \\ {}^{-\sigma_T}/_{C} & \varsigma \ge 0 \end{cases} \quad \text{(D3)}$$

where C is an ill-defined constant that was set to, $C = 2.0$, following [*Stull*, 1991; *DeBruin et al.*, 1993]. An initial evaluation of u_* and T_* can be obtained from equations (D1) and (D3) assuming neutral conditions. Next, a first evaluation of the stability parameter can be obtained by implementing (D3) in equation (7) and that of the sensible heat flux is obtained from equation (20). The process is iterated until convergence is achieved.

[68] From equation (A5), the sign of the third moment of the temperature structure function (see A1 for n = 3) and the stability parameter are the same. This makes it possible to select the corresponding similarity relationships according to stability conditions.

D1.2. Dissipation Rate for Temperature Variance

[69] From similarity theory, the dissipation rate of temperature variance can be estimated as,

$$\varepsilon_T = \left(H/\rho C_p\right)^2 \left[K(z-d)u_*\right]^{-1} \phi_{\varepsilon T}(\zeta) \quad \text{(D4)}$$

where $\phi_{\varepsilon T}(\zeta)$ is a similarity function. Following *Kiely et al.* [1996], under unstable conditions it can be expressed as

$$\phi_{\varepsilon T}(\varsigma) = \begin{cases} 0.88 & -\varsigma < 0.04 \\ 0.12(-\varsigma)^{-1/3} & 0.04 \le -\varsigma \end{cases} \quad \text{(D5)}$$

Equation (D4) is known as the temperature variance dissipation method for estimating sensible heat flux [*Brutsaert*, 1982]. Here ε_T can be determined by sequentially iterating the following equations: starting with neutral conditions: (1) The friction velocity is determined from equations (D1) and (D2). (2) The dissipation rate of turbulent kinetic energy, ε, is determined by applying similarity theory using the expression, $\varepsilon = [k(z-d)\phi_\varepsilon(\zeta)]^{-1} u_*^3$, where $\Phi_\varepsilon(\zeta)$ is $\Phi\varepsilon(\zeta) = (1 + 0.5|\zeta|^{2/3})^{2/3}$ when the stability parameter is within the range, $0 < -\zeta \le 2$. (3) The Taylor hypothesis of frozen turbulence is used to convert time series, $r = j/f$, to spatial series from $x = \bar{u}(j/f)$, where x and $\bar{u}$ denote distance and horizontal mean wind speed along the flow direction, where j is a sample lag between data points, and f is the sampling frequency. Using regression analysis for different r values, the second-order temperature structure function (defined in equation (A1) for n = 2) is then implemented as shown in equation (D6) in order to determine the dissipation rate of temperature variance,

$$S^2_{(r)} = 3.4\varepsilon_T \varepsilon^{-1/3} (\bar{u}r)^{2/3} \quad \text{(D6)}$$

where the Kolmogorov's constant for the one-dimensional temperature spectrum is set to 0.85. (4) The sensible heat flux determined after rearranging terms in equation (D4) is used to obtain the first approximated stability parameter from equation (7). The process is iterated until convergence is achieved.

D2. Method 2: Wind Velocity and Temperature Measured at High Frequency are Available

D2.1. Sensible Heat Flux

[70] For this case, the friction velocity and stability parameter required for determining the sensible heat flux estimates using the equations (17) and (20) can be directly obtained from the corresponding covariance as, $u_* = -(u'w')^{0.5}$ and $\zeta = (\text{kg}(z-d)/T)\,(w'T')\,(u'w')^{-3/2}$. Where,

u′, w′ are, respectively, the horizontal and vertical wind velocity fluctuations, and T' the temperature fluctuations.

D2.2. Dissipation Rate for Temperature Variance

[71] The mixed third-order structure function, $D_{UTT(x)}$, represents the expected value of the product of the longitudinal velocity difference and the squared temperature difference as a function of the distance along the flow direction, x. Following *Monin and Yaglom* [1981], $D_{UTT(x)} = -4/3\ \varepsilon_T x$. As described for (D6), Taylor's frozen turbulence hypothesis may be used to convert time series into spatial series. Thus ε_T can be determined from the following expression,

$$D_{UTT_{(r)}} = \frac{1}{m-j}\sum_{i=1+j}^{m}\left(u_i - u_{i-j}\right)\left(T_i - T_{i-j}\right)^2 = -4/3\varepsilon_T(\bar{u}r) \quad \text{(D7)}$$

where m is the number of data points in the 30-minute interval measured at frequency (f) in Hz and j is a sample lag between data points corresponding to a time lag ($r = j/f$). Equation (D7) is then evaluated for a range of time lags that follows the linear relationship predicted by equation (D7).

[72] **Acknowledgments.** The author gratefully acknowledges R. L. Snyder for providing all the data used in this work an also with K. T. Paw U for revision, valuable comments, and personal encouragement throughout the work. The author fully appreciates the contributions of the reviewers, whose suggestions have helped to substantially improve the original manuscript. Thanks go to Asun for her help in using various facilities at the UCD and J. Cecilia for mathematical assessment. This work was supported under project REN2001/CLI1630 and by a grant from the Spanish Ministerio de Educación, Ciencia y Tecnologia and Vicerectorat de Recerca of the Universitat de Lleida.

References

Albertson, J. D., M. B. Parlange, G. Katul, C. R. Chu, H. Striker, and S. Tyler (1995), Sensible heat flux estimates using variance methods, *Water Resour. Res.*, *31*, 969–974.

Brutsaert, W. (1975), A theory for local evaporation (or heat transfer) from rough and smooth surfaces at ground level, *Water Resour. Res.*, *11*, 543–550.

Brutsaert, W. (1982), *Evaporation Into the Atmosphere*, 299 pp., D. Reidel, Norwell, Mass.

Businger, J. A., J. C. Wyngaard, I. Izumi, and E. F. Bradley (1971), Flux profile relationships in the atmospheric surface layer, *J. Atmos. Sci.*, *28*, 181–189.

Castellví, F., P. J. Perez, and M. Ibañez (2002), A method based on high-frequency temperature measurements to estimate the sensible heat flux avoiding the height dependence, *Water Resour. Res.*, *38*(6), 1084, doi:10.1029/2001WR000486.

Cellier, P. (1986), On the validity of flux-gradient relationships above very rough surfaces, *Boundary Layer Meteorol.*, *36*, 417–419.

Cellier, P., and Y. Brunet (1992), Flux-gradient relationships above tall plant canopies, *Agric. For. Meteorol.*, *58*, 93–117.

Chen, W., M. D. Novak, T. A. Black, and X. Lee (1997a), Coherent eddies and temperature structure functions for three contrasting surfaces. Part I: Ramp model with finite microfront time, *Boundary Layer Meteorol.*, *84*, 99–123.

Chen, W., M. D. Novak, T. A. Black, and X. Lee (1997b), Coherent eddies and temperature structure functions for three contrasting surfaces. Part II: Renewal model for sensible heat flux, *Boundary Layer Meteorol.*, *84*, 125–147.

Clayson, C. A., C. W. Fairall, and J. A. Curry (1996), Evaluation of turbulent fluxes at the ocean surface using surface renewal theory, *J. Geophys. Res.*, *101*(C12), 28,503–28,513.

Danckwerts, P. V. (1951), Significance of liquid-film coefficients in gas absorption, *Indust. Eng. Chem.*, *43*, 1460–1567.

DeBruin, H. A. R., W. Kohsiek, and B. J. J. M. Van Den Hurk (1993), A verification of some methods to determine the fluxes of momentum, sensible heat and water vapor using standard deviation and structure parameter of scalar meteorological quantities, *Boundary Layer Meteorol.*, *63*, 231–257.

Foken, T., and B. Wichura (1996), Tools for quality assessment of surface-based flux measurements, *Agric. For. Meteorol.*, *78*, 83–105.

Gao, W., R. H. Shaw, and K. T. Paw U (1989), Observation of organized structure in turbulent flow within and above a forest canopy, *Boundary Layer Meteorol.*, *47*, 349–377.

Garratt, J. R. (1980), Surface influence upon vertical profiles in the atmospheric near-surface layer, *Q. J. R. Meteorol. Soc.*, *106*, 803–819.

Higbie, R. (1935), The rate of absorption of a pure gas into a still liquid during short periods of exposure, *Trans. Am. Inst. Chem. Eng.*, *31*, 355–388.

Hsieh, C., and G. Katul (1996), Estimation of momentum and heat fluxes using dissipation and flux-variance methods in the unstable surface layer, *Water Resour. Res.*, *32*, 2453–2462.

Kader, B. A., and A. M. Yaglom (1990), Mean fields and fluctuation moments in unstably stratified turbulent boundary layers, *J. Fluid Mech.*, *212, 637–662.*

Kaimal, J. C., and J. J. Finnigan (1994), *Atmospheric Boundary Layer Flows*, 289 pp., Oxford Univ. Press, New York.

Katul, G., M. Goltz, C. Hsieh, Y. Cheng, F. Mowry, and J. Sigmon (1995), Estimation of surface heat and momentum fluxes using the flux-variance method above uniform and non-uniform terrain, *Boundary Layer Meteorol.*, *74*, 237–260.

Katul, G., C. Hsieh, R. Oren, D. Ellsworth, and N. Philips (1996), Latent and sensible heat flux predictions from a uniform pine forest using surface renewal and flux variance methods, *Boundary Layer Meteorol.*, *80*, 249–282.

Kiely, G., J. D. Albertson, M. B. Parlange, and W. E. Eichinger (1996), Convective scaling of the average dissipation rate of temperature variance in the atmospheric surface layer, *Boundary Layer Meteorol.*, *77*, 267–284.

Liu, W. T., K. B. Katsaros, and J. A. Businger (1979), Bulk parameterization of air-sea exchanges of heat and water vapor including the molecular constraints at the interface, *J. Atmos. Sci.*, *36*, 1722–1735.

Lloyd, C. R., A. D. Culf, A. J. Dolman, and J. H. C. Gash (1991), Estimates of heat flux from observations of temperature observations, *Boundary Layer Meteorol.*, *57*, 311–322.

Monin, A. S., and A. M. Yaglom (1981), *Statistical Fluid Mechanics: Mechanics of Turbulence*, 2 vols., edited by J. L. Lumley, MIT Press, Cambridge, Mass.

Padro, J. (1993), An investigation of flux-variance methods and universal functions applied to three land-use types in unstable conditions, *Boundary Layer Meteorol.*, *66*, 413–425.

Paw U, K. T. (2002), Coherent structures and surface renewal, in *Advanced Short Course on Agricultural*, *Forest and Micro Meteorology*, edited by F. Rosi, P. Duce, and D. Spano, pp. 63–76, Cons. Naz. delle Ric., Rome.

Paw U, K. T., and Y. Brunet (1991), A surface renewal measure of sensible heat flux density, paper presented at 20th Conference on Agriculture and Forest Meteorology, *Am. Meteorol. Soc.*, Salt Lake City, Utah.

Paw U, K. T., Y. Brunet, S. Collineau, R. H. Shaw, T. Maitani, J. Qiu, and L. Hipps (1992), On coherent structures in turbulence within and above agricultural plant canopies, *Agric. For. Meteorol.*, *61*, 55–68.

Paw U, K. T., J. Qiu, H. B. Su, T. Watanabe, and Y. Brunet (1995), Surface renewal analysis: A new method to obtain scalar fluxes without velocity data, *Agric. For. Meteorol.*, *74*, 119–137.

Raupach, M. R., J. J. Finnigan, and Y. Brunet (1989), Coherent eddies in vegetation canopies, in paper presented at the 4th Australian Conference on Heat and Mass Transfer, Univ. of Canterbury, Christchurch, New Zealand.

Raupach, M. R., J. J. Finnigan, and Y. Brunet (1996), Coherent eddies in vegetation canopies: The Mixing-layer analogy, *Boundary Layer Meteorol.*, *78*, 351–382.

Sellers, P. J., Y. Mintz, Y. C. Sud, and A. Dalcher (1986), A simple biosphere model (SiB) for use within general circulation models, *J. Atmos. Sci.*, *43*, 505–531.

Shaw, R. H., Y. Brunet, J. J. Finnigan, and M. R. Raupach (1995), A wind tunnel study of air flow in waving wheat: Two-point velocity statistics, *Boundary Layer Meteorol.*, *76*, 349–376.

Snyder, R. L., D. Spano, and K. T. Paw U (1996), Surface renewal analysis for sensible and latent heat flux density, *Boundary Layer Meteorol.*, *77*, 249–266.

Soloviev, A. V., and P. Schlüssel (1994), Parameterization of the cool skin of the ocean and of the air-ocean gas transfer on the basis of modeling surface renewal, *J. Phys. Oceanogr.*, *24*, 1339–1346.

Spano, D., R. L. Snyder, P. Duce, and K. T. Paw U (1997), Surface renewal analysis for sensible heat flux density using structure functions, *Agric. For. Meteorol.*, *86*, 259–271.

Spano, D., R. L. Snyder, P. Duce, and K. T. Paw U (2000), Estimating sensible and latent heat flux densities from grapevine canopies using surface renewal, *Agric. For. Meteorol.*, *104*, 171–183.

Stull, R. B. (1991), *An Introduction to Boundary Layer Meteorology*, 666 pp., Kluwer Acad., Norwell, Mass.

Tillman, J. E. (1972), The indirect determination of stability, heat and momentum fluxes in the atmospheric boundary layer from simple scalar variables during dry unstable conditions, *J. Appl. Meteorol.*, *11*, 783–792.

Van Atta, C. W. (1977), Effect of coherent structures on structure functions of temperature in the atmospheric boundary layer, *Arch. Mech.*, *29*, 161–171.

Wang, J., and R. L. Bras (1998), A new method for estimation of sensible heat flux from air temperature, *Water Resour. Res.*, *34*, 2281–2288.

Weaver, H. L. (1990), Temperature and humidity flux-variance relations determined by one-dimensional eddy correlation, *Boundary Layer Meteorol.*, *53*, 77–91.

Wesson, K. H., G. Katul, and C.-T. Lai (2001), Sensible heat flux estimation by flux variance and half-order time derivative methods, *Water Resour. Res.*, *37*, 2333–2343.

Wieringa, J. (1993), Representative roughness parameters for homogeneous terrain, *Boundary Layer Meteorol.*, *63*, 323–363.

Zapata, N., and A. Martinez-Cob (2001), Estimation of sensible and latent heat flux from natural sparse vegetation surfaces using surface renewal, *J. Hydrol.*, *254*, 215–228.

F. Castellví, Department de Medi Ambient i Cienciès del Sòl, Escola Tècnica Superior Enginyeria Agrària, Universitat de Lleida, Av. Rovira Roure, 177, E-25198, Lleida, Spain. (f-castellvi@macs.udl.es)